

Financial stress and crude oil implied volatility: New evidence from continuous wavelet transformation framework



Debojyoti Das^a, Debasish Maitra^b, Anupam Dutta^{c,*}, Sankarshan Basu^a

^a Finance & Accounting Area, Indian Institute of Management Bangalore, Bengaluru, Karnataka 560076, India

^b Finance & Accounting Area, Indian Institute of Management Indore, Indore, Madhya Pradesh 45356, India

^c School of Accounting and Finance, University of Vaasa, Wolffintie 34, 65200 Vaasa, Finland

ARTICLE INFO

JEL classification:

C32
C58
G1

Keywords:

Crude oil
Crude oil implied volatility
Financial stress
Wavelet analysis

ABSTRACT

This study explores the theoretical possibility of co-movement and causality between crude oil implied volatility (OVX) and financial stress in a wavelet framework. The paper contributes to the existing literature in at least three possible ways: (a) First, the study considers not only composite financial stress indicators but also uses the categorical stress components such as Credit, Equity Valuation, Funding, Safe Assets and Volatility. (b) Second, the study employs a wavelet-based approach in tracking the co-movement and causality between oil and financial stress in a continuous time-frequency space. Lastly, (c) while previous studies mainly use oil price changes to assess the relationship with financial stress, the present study evaluates the role of forward-looking (30-days ahead) oil price uncertainty (proxied by OVX). The findings indicate the existence of co-movement between oil volatility and financial stress, mainly around the phases of economic turbulence. The patterns and strength of such co-movements are time-variant. The direction of the relationship is mostly positive, and the lead-lag relationship reveals that OVX tends to drive the relationship. It is further observed that the causalities between the variables are mostly bi-directional. However, relatively stronger causalities are transmitted from OVX towards FSI. Furthermore, the association between OVX and stress indicators is assessed in two different states of the economy, i.e., state of distress and tranquillity. The findings suggest that the causal co-movement intensifies majorly during the state of distress. Overall, the outcome of this study could be useful to policymakers and investors to anticipate the impending changes in the relationship to mitigate its potential adverse impact.

1. Introduction

The impact of crude oil price changes on the global economic order and financial markets has been well documented. A plethora of prior studies have examined the transitive relationship between oil shocks and diverse financial market segments, including equity markets (Das and Kannadhasan, 2020; Ready, 2018), bond markets (Kang et al., 2014; Tule et al., 2017), precious metals (Das et al., 2020; Uddin et al., 2018), exchange rates (Atems et al., 2015; Basher et al., 2012), interest rates (Bodenstein et al., 2013; Ioannidis and Ka, 2018) and banking institutions (Lee and Lee, 2019; Saif-Alyousfi et al., 2020). Interestingly, Chen et al. (2014) note that considering a single segment of the financial markets may not be a reliable indicator of the financial system's sensitivity to oil shocks. However, if the other segments of financial markets are not considered to examine their exposure to oil shocks, it may result

in ambiguous signals (Chen et al., 2014). Therefore, Chen et al. (2014) propose using the Financial Stress Index (FSI), a composite indicator of financial market instability. The FSI is a continuous variable with an annexing spectrum of values that depicts changing expectations of financial market losses induced by macroeconomic uncertainties (Illing and Liu, 2006).

The theoretical linkages between oil and financial stress can be driven by at least two channels: (a) the potential influences on economic activity and (b) altering sentiments of the investor (Nazlioglu et al., 2015). In the case of oil importers, the rising oil prices reduce economic activities and boost import bills, resulting in a current account deficit. The higher input cost of production with regard to higher oil prices would deplete corporate earnings and hence, falling stock prices (Wan and Kao, 2015). The expectation of a drop in oil prices, on the other hand, would upset the economic order in oil-exporting countries

* Corresponding author.

E-mail addresses: debojyoti.das@iimb.ac.in (D. Das), debasishm@iimdr.ac.in (D. Maitra), anupam.dutta@uwasa.fi (A. Dutta), sankarshan.basu@iimb.ac.in (S. Basu).

(Hammoudeh, 1988). As a result, it is difficult for lenders to determine the genuine quality of borrowers in the face of future cash flow concerns. Furthermore, lower consumer demand due to increased pricing would discourage companies from expanding their operations. Thus, the aggregate demand for credit is likely to decline, affecting the performance of the banking and financial system (Nazlioglu et al., 2015).

Another aspect of the relationship, one may argue, is that periods of financial stress are frequently connected with lower economic activity, which leads to lower energy consumption and, as a result, lower oil prices. Additionally, because oil is a marketable commodity, investors see oil-derived assets as a viable alternative to traditional financial markets. It's worth noting that the financialization of the oil market has resulted in a close relationship between oil and finance. Hence, the price of oil is determined not only by supply and demand pressures of the market but also by financial market conditions (Bianchi et al., 2020; Wan and Kao, 2015). Thus, the investors' portfolio adjustment pattern in response to the oil price movement is also an important part of the relationship. While oil prices are rising, Nazlioglu et al. (2015) believe that investors are fleeing traditional financial markets (such as shares) and flocking to the oil markets. Investors, on the other hand, tend to trade in financial markets when oil prices are down, further decreasing oil prices. As a result, the theoretical guidelines proposed by the previous studies seemingly suggest a bidirectional relationship between oil and financial stress.

This study explores the theoretical possibility of co-movement between crude oil implied volatility (OVX) and financial stress. The paper contributes to the existing literature in at least three possible ways: (a) First, while the previous literature considers only a composite FSI (Das et al., 2018b; Nazlioglu et al., 2015; Wan and Kao, 2015), the current study uses the financial stress dataset provided by the Office of Financial Research (OFR), United States (US) Department of the Treasury. The OFR provides a composite FSI and categorical bifurcations of stress components. The bifurcation refers to the classification of stress based on the financial system categories, such as Credit, Equity Valuation, Funding, Safe Assets and Volatility. Thus, this study provides additional insights with respect to the interaction of oil prices with composite as well as categorical stress indicators. (b) Second, the relationship between oil and financial stress may be characterized as a bilateral (Das et al., 2018b; Nazlioglu et al., 2015). Furthermore, depending on the nature of the event, the lead-lag mechanism between these variables can vary through time and frequency. In this case, using the wavelet coherence technique to follow the co-movement of oil and financial stress in a continuous time-frequency space is useful. The phase indicators in the wavelet coherence map can detect the lead-lag effects that change across time and frequency, which is an added benefit of employing this approach. Additionally, the causal transmission between the pair of variables is also studied in a wavelet framework. This helps to unravel the pairwise causalities across time and frequencies. Therefore, a wavelet-based technique can draw dynamic inferences, which is seldom in past literature. (c) Third, while previous studies mainly use oil price changes to assess the relationship with financial stress, the present study argues that it is equally critical to understand the role of forward-looking (30-days ahead) oil price uncertainty (proxied by OVX). The implied volatility indexes such as OVX not only contain historical information but also comprise investors' expectations about future changes in the oil market (Bouri, 2015a; Dutta, 2017; Liu et al., 2013). Hence, OVX is regarded as a better measure of oil market uncertainty (Dutta, 2017; Dutta et al., 2017; Xiao et al., 2019). In addition, the OVX also track the investor's sentiments; thus, when the fear is high, the options are priced, keeping higher volatilities into consideration than otherwise (Maghyereh et al., 2016). The fear of impending oil market risks could lead to a state of caution in the economy and financial markets. Therefore, this study explores this aspect of the relationship, which is not investigated adequately in the past literature (with the limited knowledge of the authors). The findings of the study could be useful to the participants in the financial markets to derive implications

for portfolio adjustments.

Uncertainty in crude oil prices has a significant influence on the economy and financial markets (Gong and Lin, 2018a; Wang and Li, 2021). Higher degrees of oil price uncertainty reflect intense or unstable oil markets. Under impending oil uncertainties, the economic agents are likely to postpone or terminate several decisions of economic interest, such as investment, production, and propensity to consume beyond others (Xie et al., 2021). Therefore, the instability in oil prices would invariably result in unfavourable economic or financial implications (You et al., 2017). Since oil uncertainty and financial stress tend to move in tandem, a positive relationship can be predicted.¹ Traditionally, exploring the relationship between oil and financial market segments has been a matter of considerable interest. However, the oil uncertainties reaching a historical high during the COVID-19 episode have renewed the interest of scholars on this topic (Corbet et al., 2020; Dutta et al., 2021, 2020; Szczygielski et al., 2021; Xie et al., 2021). Despite this, few of this research look at the link between OVX and FSI. Further, deriving the historical and contemporaneous relationship between OVX and categorical stress indicators offers additional value to the existing literature and market participants in general. This serves as the prime motivation for this study.

The findings indicate the existence of co-movement between oil volatility and financial stress, mainly around the phases of economic turbulence. The patterns and strength of such co-movements are time-variant. The direction of the relationship is mostly positive, and the lead-lag relationship reveals that OVX tends to drive the relationship. It is further observed that the causalities between the OVX and categorical FSIs are also mostly bi-directional. However, relatively stronger causalities are transmitted from OVX. Furthermore, the OVX and stress indicators are decomposed into two different states of the economy, i.e., the state of distress and the state of tranquillity. The results suggest that the causalities mainly exist in the state of distress. Thus, this relationship must be given due attention, especially during the phases of economic downturns. The rest of the paper is structured as follows: Section 2 reviews the relevant literature, Section 3 describes the data, Section 4 discusses the methodology, Section 5 elaborates on the empirical findings, Section 6 scrutinizes the causal association among OVX and region-specific stress indexes, Section 7 reports the results of the robustness analysis, and Section 8 concludes.

2. Literature review

The instability of crude oil prices transmits financial market uncertainties and negative shocks to the global economy (Das and Kannadhasan, 2020; Dutta et al., 2017; Gong and Lin, 2018b, 2018a). Past studies that examine the impact of oil prices on different segments of the financial market (such as equities, bonds, precious metals, and other commodities, among others) are available in abundance. In the context of equity markets, Ma et al. (2019) contend that the theoretical association between oil and equity markets is backed by substantial empirical support worldwide. For instance, the pioneering study by Jones and Kaul (1996) found a negative impact of oil on the equity indexes of the developed country. Several subsequent research deliberations using methodological approaches such as quantile regression (QR), Vector Autoregression (VAR), and Capital Asset Pricing Model (CAPM) also support this claim (for instance, see Basher et al., 2012; Cunado and de Gracia, 2014; Lee and Zeng, 2011; Sadorsky, 1999). By contrast, some papers posit a positive association between oil and equity (Arouri and Rault, 2012; El-Sharif et al., 2005; Kilian and Park, 2009; Narayan and Narayan, 2010). Some studies further argue that the direction and

¹ Regarding the direction of relationship, Xiao et al., 2019 also find a significantly positive association between OVX and Chinese stock implied volatility index (VXFXI). Further, the preliminary tests such as 'decile analysis' in section 2, also affirm the positive OVX-FSI association.

Table 1

Definition of categorical stress indicators given by the Office of Financial Research.

Category	Definition
Credit	"Contains measures of credit spreads, which represent the difference in borrowing costs for firms of different creditworthiness. In times of stress, credit spreads may widen when default risk increases or credit market functioning is disrupted. Wider spreads may indicate that investors are less willing to hold debt, increasing costs for borrowers to get funding." Variables used: BaML Corporate Master, BaML High Yield Corporate Master, BaML Euro Area Corp Bond Index, BaML Euro Area High Yield Bond Index, JP Morgan CEMBI Strip Spread, JP Morgan EMBI Global Strip Spread.
Equity Valuation	"Contains stock valuations from several stock market indexes, which reflect investor confidence and risk appetite. In times of stress, stock values may fall if investors become less willing to hold risky assets." Variables used: MSCI Emerging Markets Index, MSCI Europe Index, NIKKEI 225 Index, S&P 500 Index.
Funding	"Contains measures related to how easily financial institutions can fund their activities. In times of stress, funding markets can freeze if participants perceive greater counterparty credit risk or liquidity risk." Variables used: 2-Year EUR/USD Cross-Currency Swap Spread, 2-Year US Swap Spread, 2-Year USD/JPY Cross-Currency Swap Spread, 3-Month EURIBOR-EONIA, 3-Month Japanese LIBOR-OIS, 3-Month LIBOR-OIS.
Safe Asset	"Contains valuation measures of assets that are considered stores of value or have stable and predictable cash flows. In times of stress, higher valuations of safe assets may indicate that investors are migrating from risky or illiquid assets into safer holdings." Variables used: 4-Week US Treasury Bill, 10-Year US Treasury Note, 10-Year German Bond, US Term Spread, US Dollar Index, Gold/USD Real Spot Exchange Rate.
Volatility	"Contains measures of implied and realized volatility from equity, credit, currency, and commodity markets. In times of stress, rising uncertainty about asset values or investor behaviour can lead to higher volatility." Variables used: CBOE S&P 500 Volatility Index, Dow Jones EURO STOXX 50 Volatility Index, ICE Brent Crude Oil Futures, Implied Volatility on 6-Month EUR/USD Options, Implied Volatility on 6-Month USD/JPY Options, JP Morgan Emerging Market Volatility Index, Merrill Lynch Euro Swaptions Volatility Estimate, Merrill Lynch US Swaptions Volatility Estimate, NIKKEI Volatility Index.

The Table defines the categorical stress indicators given by the Office of Financial Research.

nature of the oil-equity relationship depend upon whether the index belongs to an oil-importing or exporting country (Das et al., 2022b; Mokni, 2020) besides the sectoral variations are also relevant (Das and Kannadhasan, 2020; Tiwari et al., 2018b; Xiao et al., 2018). In addition,

other studies different spheres of the financial market, such as for bond markets (Dai and Kang, 2021; Kang et al., 2014), precious metals (Charlot and Marimoutou, 2014; Das et al., 2020; Umar et al., 2021), exchange rates (Albulescu and Ajmi, 2021; Atems et al., 2015; Beckmann et al., 2020), and other commodities (Ahmed and Huo, 2021; Maitra et al., 2021).

The aforementioned studies majorly explore the relationship between financial market segments with respect to changes in oil prices (or shocks based on structural VAR models). However, another strand of literature highlights the role of oil volatility on the financial market returns and volatility. For instance, using the Multivariate Generalized Autoregressive Conditional Heteroskedasticity (MGARCH) model, Malik and Hammoudeh (2007) report evidence of significant volatility spillover between oil and equity markets in the US and Gulf region. In a similar context, using a bivariate GARCH approach, Malik and Ewing (2009) examine the volatility transmission across five different equity sectors in the US and report supporting evidence. Arouri et al. (2011) employ a generalized VAR-GARCH framework to study the volatility transmission between oil and sectoral-level equity indexes in the US and Europe. The authors conclude that the spillover is bidirectional in the case of equity markets in the US, however, only unidirectional spillover from oil markets is evident in the case of European markets. Bouri (2015b) also uses the VAR-GARCH model to disentangle the return and volatility spillover between oil and Lebanese equity markets and suggests intensified spillover from oil markets during the financial crisis of 2007. Using realized volatility (RV) measure and the Diagonal-BEKK model, Boldanov et al. (2016) observe the correlation between oil and equity market volatility across oil-importing and exporting countries. Wang et al. (2018) use an RV and predictive regression-based design to explore whether the oil volatility predicts equity volatility. The authors

Table 2

Unconditional correlation of financial stress indexes with OVX.

	a. Full sample	b. GFC 2007–09	c. COVID-19
FSI	0.2710	0.3264	0.6837
Credit	0.1945	0.2240	0.6296
EV	0.2541	0.3146	0.6211
SA	0.1260	0.1463	0.4995
Funding	0.0767	0.1066	0.5016
Volatility	0.2842	0.3761	0.6121
Observations	3622	397	42

The table reports the results for the unconditional (Pearson) correlation between OVX and stress indexes for the full sample and two recession-affected subsamples: (a) US subprime crisis dating from December 2007 till June 2009, and (b) COVID-19 covering from February to April 2020.

Fig. 1. Crude oil implied volatility and composite financial stress index.

The figure plots the historical data for crude oil implied volatility index (OVX) and the composite financial stress index (FSI) provided by the OFR for the period starting from May 10, 2007 to September 28, 2021. The grey shaded areas are the recessionary phases determined by NBER. The first phase spans from December 2007 till June 2009 which relates to the period of US subprime crisis. COVID-19 determines the second recessionary phase spanning from February to April 2020.

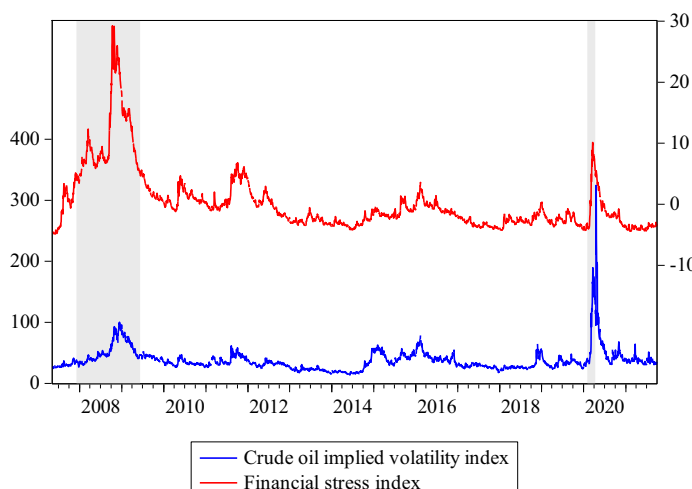


Table 3
Decile-based analysis.

Decile	OVX	FSI	Credit	EV	SA	Funding	Volatility
1st	19.5592	-3.886	-0.8077	-0.845	-0.3878	-0.8502	-2.1177
2nd	25.4551	-3.3192	-0.5837	-0.4966	-0.2435	-0.6051	-1.7584
3rd	28.5116	-2.8274	-0.4302	-0.3894	-0.1596	-0.4806	-1.4492
4th	30.9623	-2.2489	-0.2832	-0.3035	-0.1102	-0.3667	-1.1753
5th	33.1073	-1.6434	-0.1531	-0.2249	-0.0479	-0.2756	-0.8828
6th	35.6083	-0.8613	0.0304	-0.1353	0.0269	-0.1365	-0.6039
7th	39.0688	0.1084	0.208	-0.0107	0.0948	0.113	-0.2739
8th	42.9183	1.18	0.5462	0.1641	0.1769	0.4844	0.1969
9th	48.4559	3.9486	1.2567	0.4416	0.2722	1.1688	0.9228
10th	77.4254	11.9766	4.2129	1.2679	0.4995	3.4996	3.4494
Decile 10th -1st	57.8662	15.8626	5.0206	2.1129	0.8873	4.3498	5.5671
Decile 9th -2nd	23.0008	7.2678	1.8404	0.9382	0.5157	1.7739	2.6812

In the table OVX is sorted into ten deciles. 1st decile denotes low oil volatility, whereas, the 10th decile corresponds to high volatility. For each of the OVX deciles, the corresponding averages of stress indexes are reported. The negative values of stress indexes ($FSI < 0$) represent relatively stable financial market conditions. The table shows that the lower (higher) values of OVX correspond to lower (higher) values of stress indexes implying a positive association. The last two rows show the differences between decile 10-1 and 9-2, respectively.

Table 4
Descriptive statistics.

	Δ OVX	Δ FSI	Δ Credit	Δ EV	Δ SA	Δ Funding	Δ Volatility
Mean ($\times 100$)	0.2488	0.0305	0.0237	0.0017	-0.0073	-0.0019	0.0235
Median	-0.1100	-0.0230	-0.0030	-0.0030	0.0000	-0.0010	-0.0100
Maximum	130.2200	3.4540	0.7310	0.6340	0.1840	1.5000	2.1780
Minimum	-90.6100	-2.8400	-0.5400	-0.5570	-0.2250	-1.1020	-1.4910
Std. Dev.	4.4183	0.3197	0.0505	0.0684	0.0279	0.0816	0.1749
Skewness	5.9603	1.6839	2.4869	0.3618	-0.1151	2.2566	2.0834
Kurtosis	381.4166	27.4494	44.9532	15.2876	8.0321	90.5775	27.9665
Jarque-Bera	21,632,574.00	91,925.53	269,356.80	22,865.28	3829.52	1,160,578.00	96,690.36
Probability	0.0000	0.0000	0.0000	0.0000	0.0000	0.0000	0.0000
Observations	3622	3622	3622	3622	3622	3622	3622

The table reports the summary statistics of all the variables considered in the study at their respective first-differences. The critical value of Jarque–Bera test at 5% level is 5.99. The Jarque–Bera test statistic confirms that the underlying characteristics of these variables depart from the assumption of normality.

Table 5
Unit root tests.

Variables at the first difference ($I(1)$)

	Intercept	ADF t-statistics	Critical value at 5%	PP Adj. t-statistics	Critical value at 5%	KPSS LM-statistics	Critical value at 5%
OVX	-9.7699***	-2.8621	-66.4116***	-2.8621	0.0156	0.4630	
FSI	-15.5793***	-2.8621	-51.0696***	-2.8621	0.0763	0.4630	
Credit	-11.7771***	-2.8621	-53.3576***	-2.8621	0.1143	0.4630	
EV	-52.8640***	-2.8621	-52.6308***	-2.8621	0.0202	0.4630	
SA	-60.5385***	-2.8621	-60.5374***	-2.8621	0.0267	0.4630	
Funding	-14.3688***	-2.8621	-46.5227***	-2.8621	0.0516	0.4630	
Volatility	-53.9815***	-2.8621	-53.9517***	-2.8621	0.0413	0.4630	

***denotes statistical significance at 1% level. The null hypothesis for ADF and PP test assume that the underlying time series has a unit root against the alternative hypothesis of stationarity. In the case for KPSS test, the null hypothesis is the underlying variable is stationary. Thus, when the LM-statistic of KPSS does not reject the null hypothesis, it means the series is stationary.

report that oil volatilities encompass additional information to traditional macroeconomic variables and can predict equity market volatilities. [Gong et al. \(2021\)](#) recently evaluated spillover of oil volatility to natural gas futures markets by applying the time-varying-parameter VAR model with stochastic volatility (TVP-VAR-SV) and Diebold–Yilmaz spillover ([Diebold and Yilmaz, 2012, 2009](#)) approach. The paper finds evidence of spillover from the oil markets; however, the spillover reduces sharply onset of the shale oil revolution.

While these mentioned studies mainly derive the volatility of oil prices using GARCH-based or RV models, an emerging stream of contemporaneous research promulgates the use of OVX. The GARCH-based or RV models provide volatilities obtained from past price data, thus, contain only historical information and limited implications for impending market risks. A forward-looking index like OVX comprise

higher information content in terms of both historical and futuristic market expectations ([Bouri et al., 2018; Dutta, 2017; Liu et al., 2013](#)). Therefore, scholars are increasingly embracing its relevance in the sphere of financial/economic research ([Dutta et al., 2017; Xiao et al., 2019, 2018](#)). For instance, employing the Autoregressive Distribution Lag (ARDL) model [Liu et al. \(2013\)](#) study the transmission of implied volatility across oil (OVX), exchange rates (EVZ), gold (GVZ) and equity markets (VIX) and suggest significant spillover in the short-run. Similarly, [Maghyereh et al. \(2016\)](#) using the spillover directional measure propounded by Diebold and Yilmaz examine transmission of volatility between OVX and implied volatility of 11 equity markets. The results suggest that spillover is largely transmitted from oil to equity markets. [Bouri et al. \(2017\)](#) study the cointegration and non-linear causality between OVX, GVZ and the implied volatility index of the Indian equity

Table 6
VAR Granger-causality test.

Null hypothesis (H_0)	MWALD statistics	Decision
FSI does not Granger cause OVX	55.3886***	Reject H_0
OVX does not Granger cause FSI	26.2216***	Reject H_0
Credit does not Granger cause OVX	55.4636***	Reject H_0
OVX does not Granger cause Credit	25.2959***	Reject H_0
EV does not Granger cause OVX	45.6846***	Reject H_0
OVX does not Granger cause EV	42.3621***	Reject H_0
SA does not Granger cause OVX	5.8524	Accept H_0
OVX does not Granger cause SA	10.0468	Accept H_0
Funding does not Granger cause OVX	16.5004**	Reject H_0
OVX does not Granger cause Funding	8.5511	Accept H_0
Volatility does not Granger cause OVX	73.115***	Reject H_0
OVX does not Granger cause Volatility	35.8109***	Reject H_0

***, ** denote statistical significance at 1% and 5% level, respectively.

market (Indian VIX) using ARDL bound and Kyrtsov-Labys nonlinear symmetric and asymmetric non-causality test. The findings suggest a significant positive impact of OVX, and GVZ on the Indian VIX. [Bašta and Molnár \(2018\)](#) detect the time-frequency co-movement by applying wavelet analysis between oil and equity markets using their corresponding implied and realized volatilities. The study reports conclusive evidence in the case of implied volatility co-movement, which is time-varying and strongly varies in timescale. [Dutta \(2018\)](#) finds evidence of both long and short-run association between OVX and US energy sector implied equity volatility index (VXXLE) employing ARDL bound tests. [Xiao et al. \(2019\)](#) examine the asymmetric and lagged impacts of OVX on the Chinese equity market implied volatility index (VXFXI) using the QR technique and assert standing evidence for the same. [Lu et al. \(2020\)](#) evaluate the forecasting ability of OVX to predict the Chinese crude oil futures market volatility utilising the Markov-regime mixed data sampling (MS-MIDAS) model. The findings confirm the predictive ability of OVX towards the Chinese crude oil futures market volatility, especially in the mid and long-term horizons.

Though a sizeable amount of recent literature focuses on the association between OVX and volatility in the financial market segments, none of the studies focuses on the relationship of OVX with composite and categorical FSI. In general, the literature concerning crude oil and financial stress is nascent since financial stress is a relatively new concept. Nevertheless, few studies in the last decade have indicated the relevance of understanding the oil and FSI relationship. [Chen et al. \(2014\)](#) study the relationship between structural oil shocks and Kansas City FSI using the SVAR framework initially suggested by [Kilian \(2009\)](#). The results show that financial shock is a crucial factor in determining oil prices, and it varies across time horizons. Hence, the authors posit that policymakers must consider the existent financial condition while understanding the influences of the oil shocks. [Nazlioglu et al. \(2015\)](#) study the volatility spillover between oil and the FSI provided by the Federal Reserve of Cleveland using the causality-in-variance and VAR research design. The authors conclude the existence of volatility transmission among the variables, mainly in the long-term time horizon. [Wan and Kao \(2015\)](#) explore the role of financial stress in mediating the relationship between oil and different financial variables using the structural threshold VAR (STVAR) model. The study finds that the interaction between oil and financial markets intensifies during the stress regime, further, the relationship is also nonlinear. Applying the QR technique, [Reboredo and Uddin \(2016\)](#) assess the impacts of FSI (proxied by St. Louis FED FSI) and economic policy uncertainty (EPU) on the energy and metal commodity futures and report a statistically significant lagged relationship in the intermediate and upper quantiles. [Das et al. \(2018b\)](#) explore the dependence structure of stocks, gold and crude oil with financial stress (St. Louis FED FSI) using the causality-in-quantile technique. The results of the study confirm bilateral causality

between oil, gold, and crude oil. [Gupta et al. \(2019\)](#) use a news-based indicator of financial stress developed by [Püttmann \(2018\)](#) and examine its role in predicting oil market movements considering the DCC-MGARCH model. The study finds evidence of strong predictability from FSI to oil returns and volatility. [Gkillas et al. \(2020\)](#) analyse the predictive ability of FSI provided by OFR for the US, emerging and other advanced economies towards the oil price volatility by employing the Heterogeneous Autoregressive-RV (HAR-RV) model. The results establish that the FSI improves the oil market volatility forecasts and highlights the contextual relevance of FSI under different forecaster's loss functions. [Liu et al. \(2021\)](#) decompose the oil price returns into structural shocks following the process of [Ready \(2018\)](#) and observe its impact on the Chinese financial stress index constructed by the authors. Applying the Markov Regime-Switching (MRS) model, the authors posit that supply-side shock is the driver of Chinese financial stress in the low-volatility regime. [Pang et al. \(2021\)](#) study whether the world or US-specific FSI given by the OFR can predict the oil realized volatility employing the MS-MIDAS model. The study concludes that the US-specific FSI is more efficient in predicting oil volatility than the world FSI. Recently, [Apostolakis et al. \(2021\)](#) studied the connectedness of financial stress of G7 countries considering stress indexes created by authors using different financial variables with EPU and Brent oil market applying the [Diebold Yilmaz \(2014, 2012\)](#) framework. The findings suggest that oil uncertainty is mainly linked with the financial stress in some G7 countries rather than the EPU. Further, the spillover is stronger in the phases of turbulences, such as the Global Financial Crisis (GFC) and the COVID-19 pandemic. More recently, [Das et al., 2022a](#) examined the role of OVX in predicting financial stress in emerging markets and found that there is a positive association between them. Further, the relationship intensifies during the phases of economic turbulence.

3. Data

The association between OVX and FSI is studied for the period commencing from May 10, 2007, through September 28, 2021. The starting point of the data is determined by the oldest availability of OVX values. The OVX data is published by Chicago Board Options Exchange (CBOE) and is availed from St. Louis FRED database. The financial stress-related indexes are sourced from the website of the OFR, U.S. Department of the Treasury, Washington DC. The study uses data at the daily frequency to capture dynamic interactions between OVX and FSI. Considering daily data is an appropriate choice as the study aims to examine the contagious behaviour among the variables. Contagion due to exogenous shocks lasts for a short span of time, and the correlation withers away in a matter of days ([Gallegati, 2012; Reboredo and Rivera-Castro, 2014](#)). Thus, daily data seems pertinent in this research setup where the relationship is transient.

While previous research has primarily focused on the relationship between crude oil and the aggregate financial stress index, one of the most important advantages of using the OFR stress index is that it provides categorical stress indicators. In addition to the aggregate financial stress index, OFR decomposes the composite index into five sub-indexes: (a) Credit, (b) Equity valuation (EV), (c) Safe assets (SA), (d) Funding, and (e) Volatility. Therefore, in addition to the headline index, the study also examines the relationship between OVX and categorical stress indexes. The stress indexes are constructed considering relevant financial/economic variables that were chosen based on an academic literature survey. After balancing the selected variables across the markets, asset classes and economy types, quantitative tests are conducted to filter redundant information. The first loading vector is then estimated using historical data from the previous 500 days and constrained Principal Component Analysis (PCA). Furthermore, the most recent data is standardized compared to all previous data. Finally, FSI is derived as the

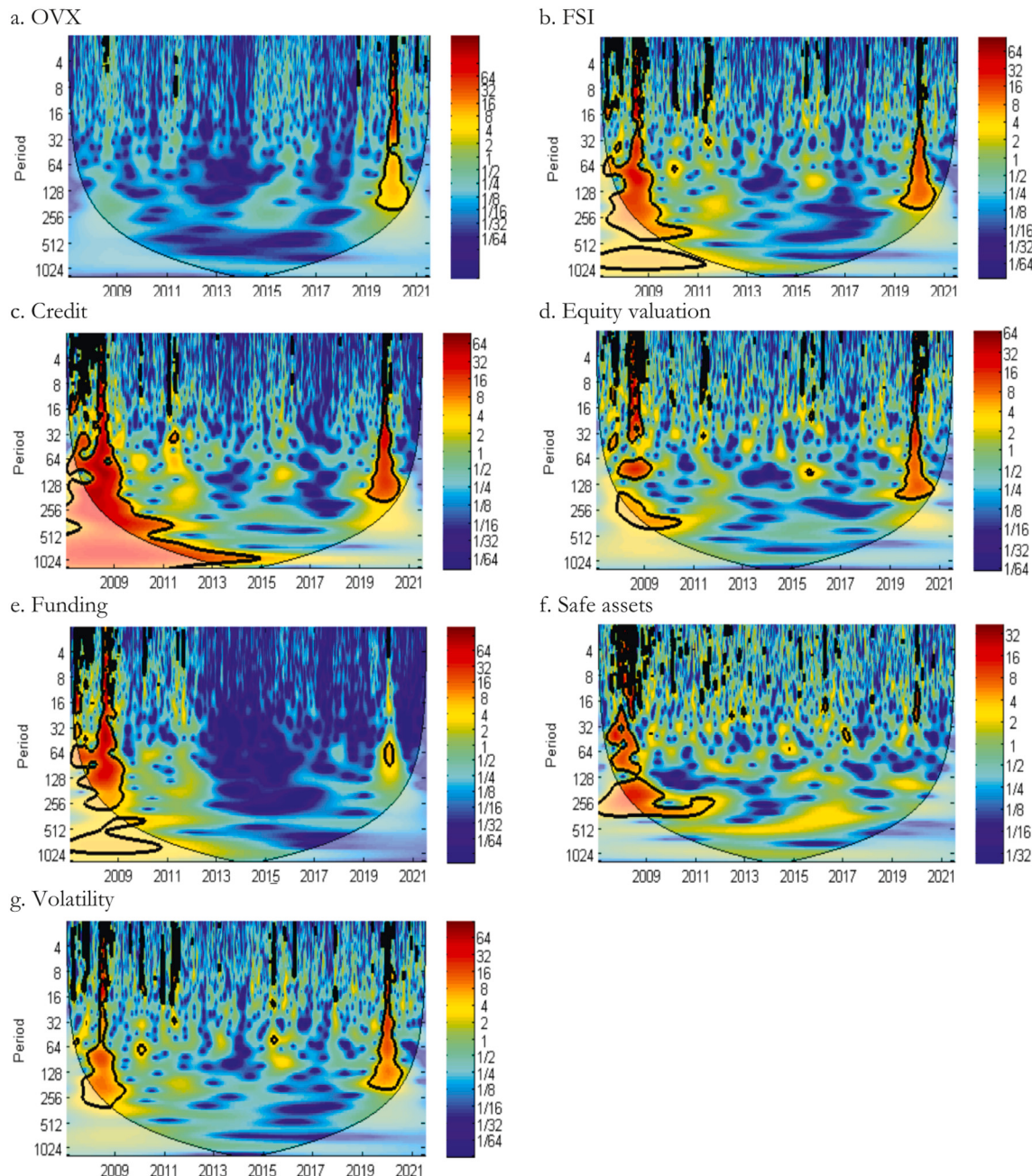


Fig. 2. Wavelet power spectrum.

The figures above represent the WPS plots for all the variables under consideration. The cone-of-influence (COI) is depicted by the *black funnel-shaped line*, which demarcates the zones affected by edge effects. The bold *black* contours on the maps denote the significant zones at 5% level. The horizontal axis determines the timeline and the vertical axis represent the frequencies in number of days. The colour bar denotes the strength of the power ranging from low to high indicated by *blue* to *red* colours, respectively. (For interpretation of the references to colour in this figure legend, the reader is referred to the web version of this article.)

scalar projection of standardized data onto the first loading vector.² The representative value of the indexes are the marginal contributions of each variable that characterize the current state of market shocks and contemporary within-variable interactions. The indexes depict a positive value when the positive contributions to the condition of financial stress exceed negative contributions and vice-versa. The indexes tend to

zero when the market variables strike at their respective long-run averages. The official definition of the categorical stress indicators and the variables used to construct these indexes is exhibited in Table 1.

Fig. 1 depicts the historical evolution of OVX and FSI during the sample interval. A visual interpretation of these indexes suggests that OVX and FSI tend to move in tandem conventionally. The grey-shaded zones indicate the recession cycles identified by the National Bureau of Economic Research (NBER). The full sample is affected by two recessionary phases. The first phase covers the period from December 2007 to June 2009, corresponding to the GFC. In contrast, the economic slowdown due to COVID-19 determines the second recessionary phase in the sample spanning from February to April 2020. It is worth noting that

² Description on the construction of the stress indexes is available at: <https://www.financialresearch.gov/working-papers/2017/10/25/the-ofr-financial-stability-index/>. Interested readers are requested to follow the aforementioned link for a detailed discussion.

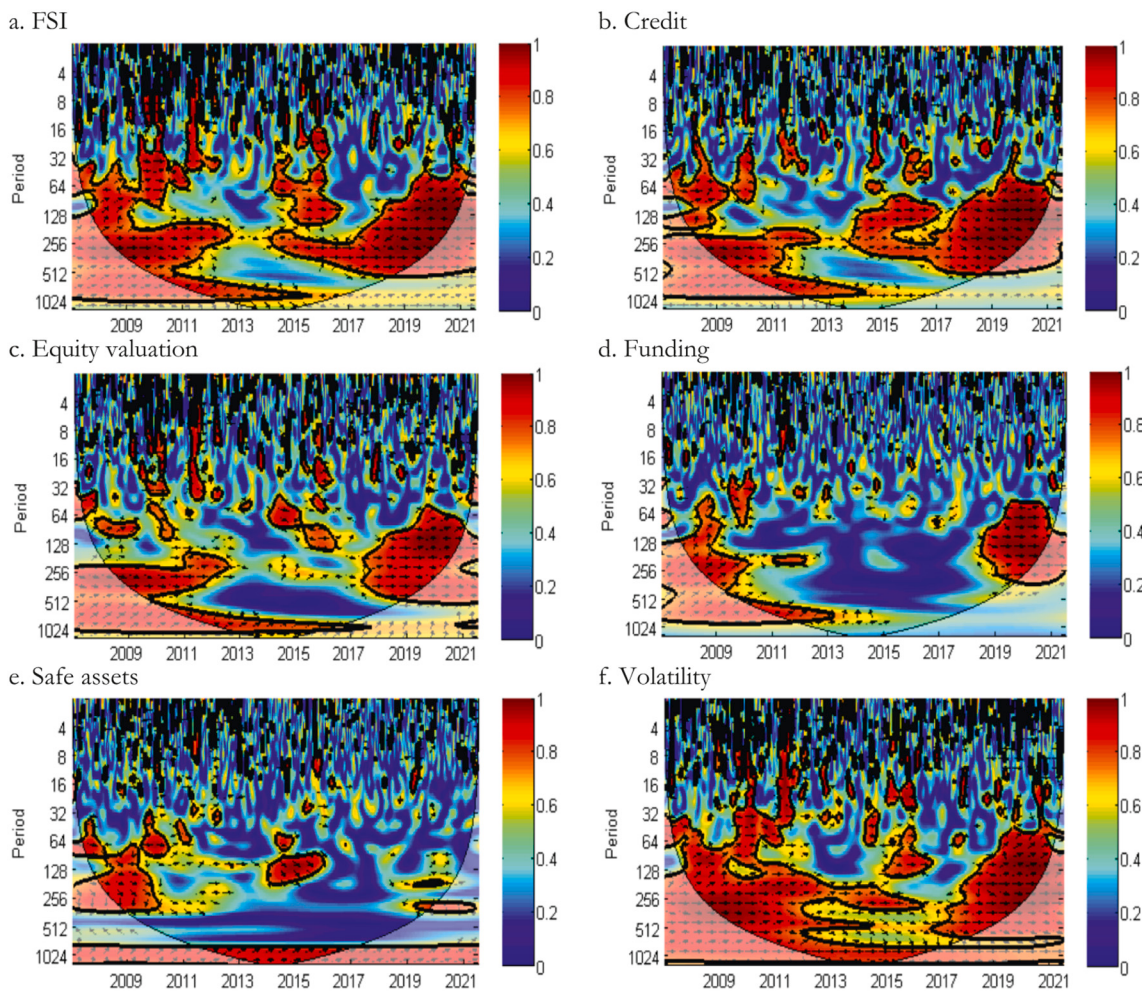


Fig. 3. Wavelet coherence maps.

The figures above represent the wavelet coherence maps for all the stress indexes paired with OVX. The COI is depicted by the *black funnel-shaped line*, which demarcates the zones affected by edge effects. The bold *black contours* on the maps denote the significant zones at 5% level. The horizontal axis determines the timeline and the vertical axis represent the frequencies in number of days. The colour bar denotes the strength of the power ranging from low to high indicated by *blue* to *red* colours, respectively. The phases are indicated by arrows. (For interpretation of the references to colour in this figure legend, the reader is referred to the web version of this article.)

the two series appear to co-move strongly during the phases of uncertainty. Interestingly, the sharpest peak for FSI is observed around GFC 2007–09, as the crisis typically involved fluctuations in the financial sector. The historical volatility peak for crude oil is observed during the phase of COVID-19. The attributable underlying reasons are nationwide lockdowns in many countries, travel bans and intermittent industrial shutdowns as safety measures.

Table 2 reports the unconditional correlations between OVX and stress indexes. The results for the full sample are reported in the first column. The weakest correlation is observed in the case of funding-related stress. Whereas the strongest correlation is observed for Volatility stress of the currency, equity, credit, and commodity markets with OVX. The second and third column of Table 1 suggests that the correlations intensify during GFC 2007–09 and intensifies further during COVID-19, respectively. The phenomenon of higher correlations between markets during the crisis periods is consistent with the ‘contagion’ hypothesis, which is well documented in the extant literature (see Bekaert et al., 2014; Kivimäki et al., 2014).

Table 3 reports the results of decile-based analysis for OVX, FSI and the categorical stress indexes. In this table, the OVX is segregated into ten deciles. The lower deciles determine the periods of low oil volatility, while the higher deciles indicate the phases of high oil volatility. The corresponding columns exhibit deciles of the composite FSI and

categorical stress indicators. The table reveals that the lower (higher) values of OVX correspond to lower (higher) values of stress indexes. Therefore, values of the stress indexes mapped with respect to OVX follow an ascending order implying a positive association between them. This is in concurrence with the theoretical guideline that suggests a positive relationship between oil prices and the financial stress (Chen et al., 2014; Das et al., 2018b; Nazlioglu et al., 2015). Thus, the study finds some preliminary support for the theoretical connotation.

The statistical properties of all the variables at their first differences are reported in Table 4. The average value (mean) of changes in OVX is higher than the changes in the headline FSI and categorical indexes thereof. The average volatility in oil prices is higher than the average changes in financial stress. Within the categorical stress indexes, the Credit sector shows highest positive value implying maximum origination of stress in this sector. The sectors SA and Funding show negative average stress values indicating the persistence of low-stress periods in these sectors. The standard deviation of OVX is the highest of all variables signifying a wavering nature of this index. The variables under consideration mostly show a positive skewness depicting more frequent occurrences of positive values, with SA being the only exception. The negative skewness of SA denotes subdued stress in this sector. Further, the kurtosis coefficient shows excess kurtosis than desired for normal distribution. Lastly, the Jarque-Bera statistic illustrates the non-

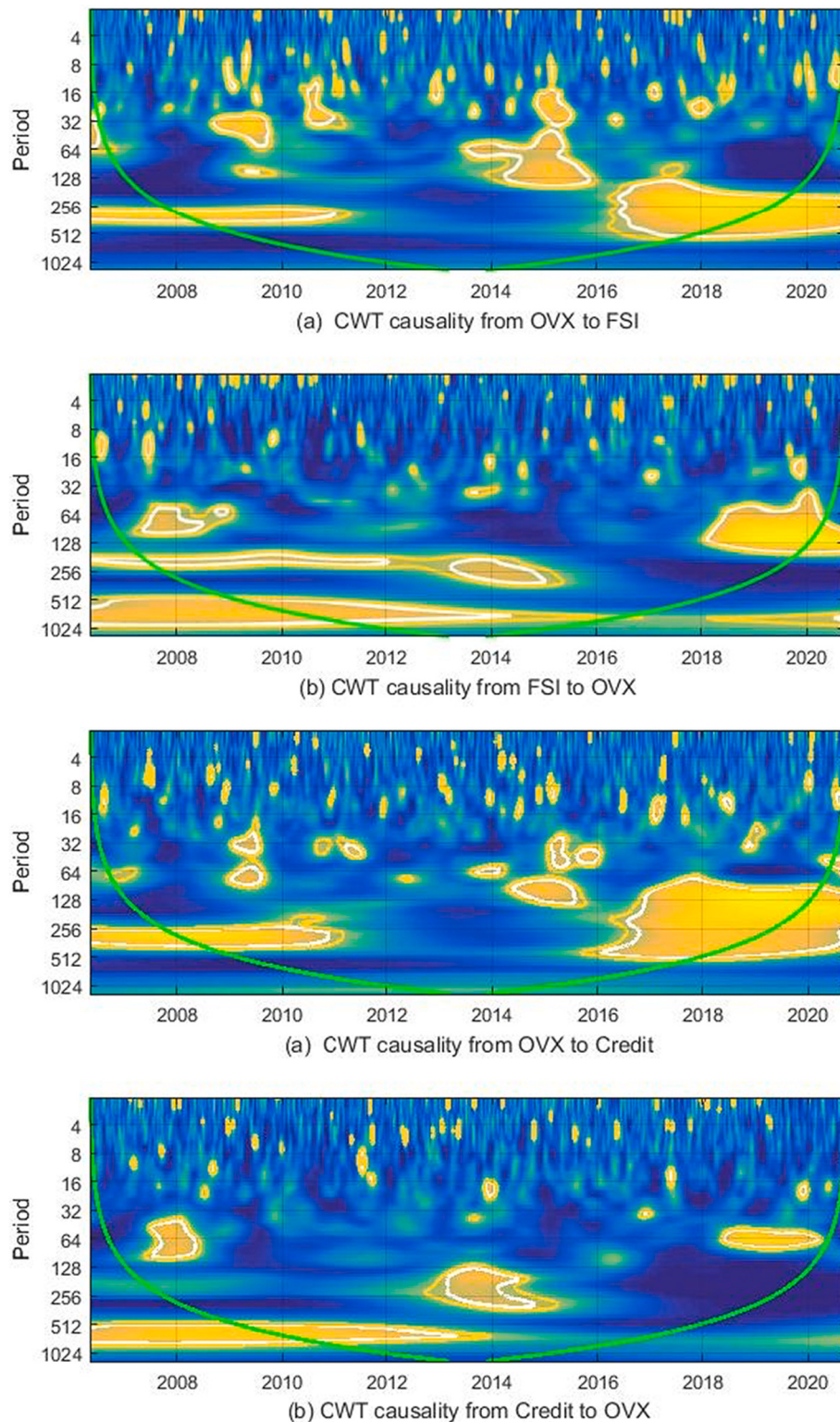


Fig. 4. a. Continuous wavelet transform plot of causality between OVX and composite FSI.

b. Continuous wavelet transform plot of causality between OVX and Credit.

c. Continuous wavelet transform plot of causality between OVX and EV.

d. Continuous wavelet transform plot of causality between OVX and Funding.

e. Continuous wavelet transform plot of causality between OVX and SA.

f. Continuous wavelet transform plot of causality between OVX and Volatility.

Note: The White and Yellow contours in sub-figures (a) and (b) represent the statistical significance at 5% and 10%, respectively. The significance levels are derived on 3000 Monte-Carlo simulation draws estimated on ARMA (1,1) null of no statistical significance. The COI is depicted by the green line, which demarcates the zones affected by edge effects. The scale has been transformed to a period for the Morlet wavelet function. Using $\omega_0 = 6$ for the optimal balance (Torrence and Compo, 1998), we have $Ft = 1.033$. s.

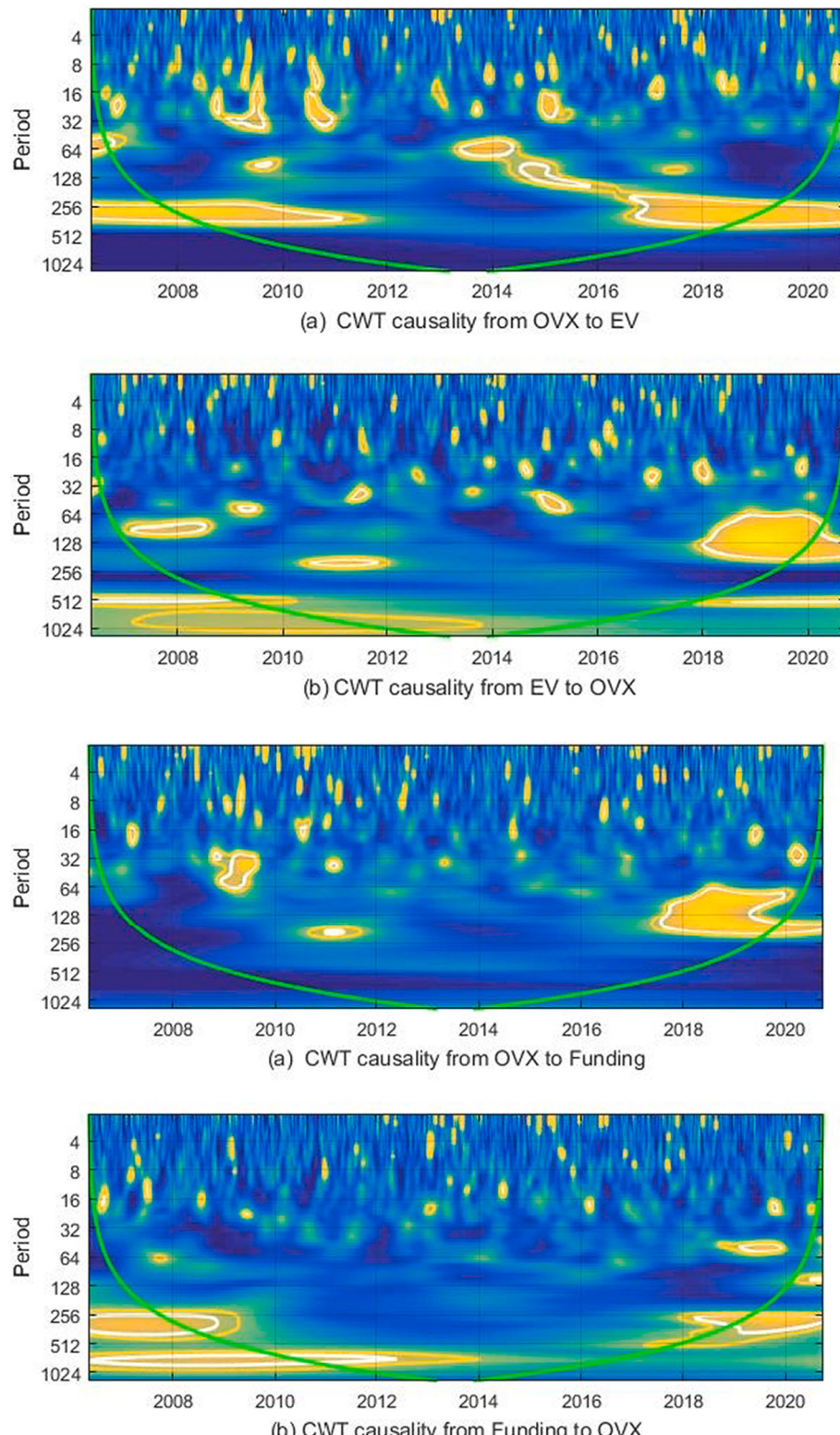
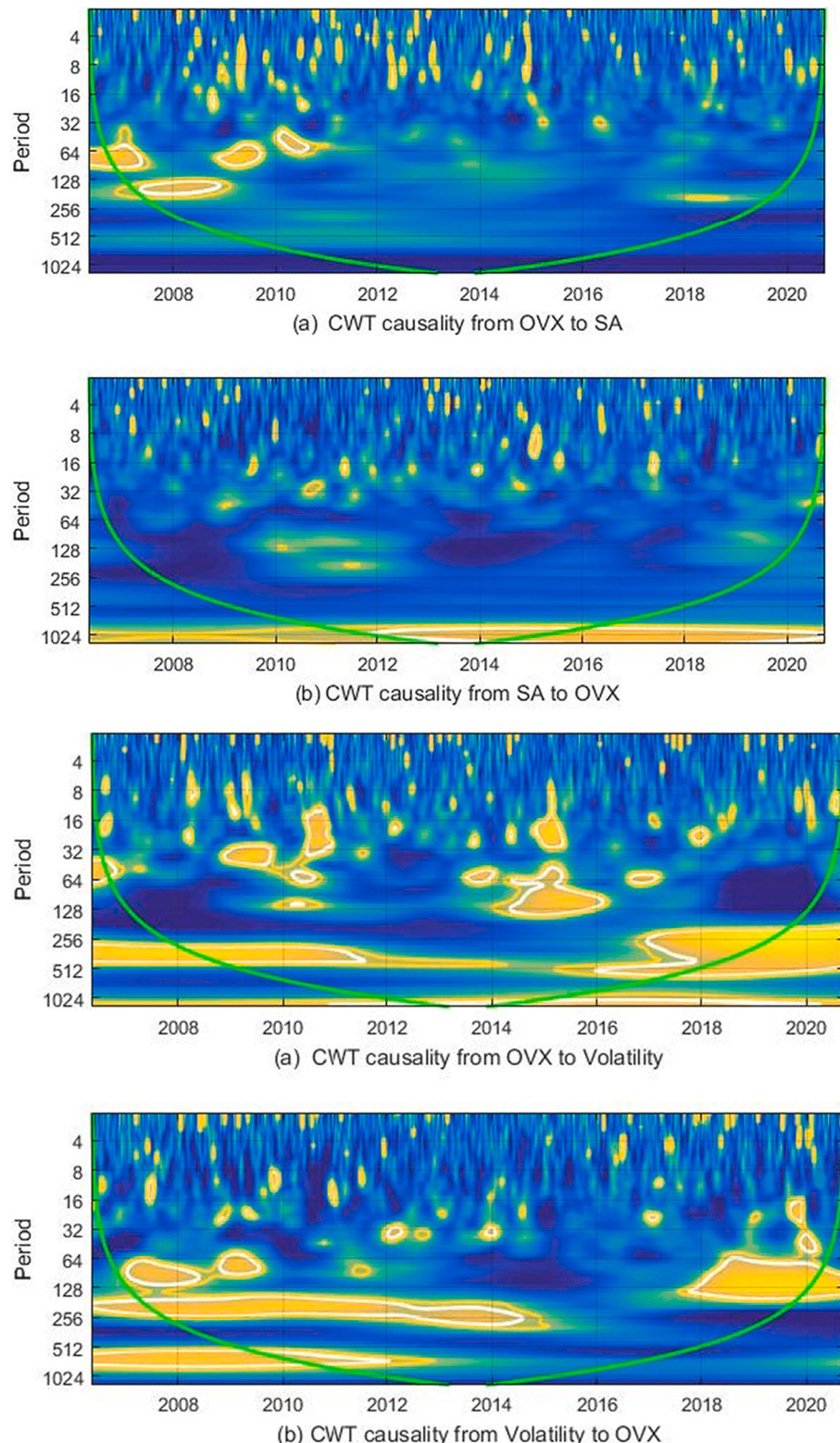


Fig. 4. (continued).

normality of all the indexes.

Table 5 exhibits the unit root tests for OVX and stress indexes. The unit root tests conducted in this study include the Augmented Dickey-Fuller (ADF) test (Dickey and Fuller, 1979), Phillips Perron (PP) test (Phillips and Perron, 1988), and Kwiatkowski, Phillips, Schmidt and Shin (KPSS) test (Kwiatkowski et al., 1992). While the null hypothesis

for ADF and PP test assumes that the underlying time series has a unit root against the alternative hypothesis of stationarity, the reverse is the case for the KPSS test. The lag length for the test is selected with reference to the Schwarz Information Criterion (SIC). The results suggest that the null hypothesis of unit root is rejected for ADF and PP test, and the alternative hypothesis stationarity is accepted. Corollary to ADF and

**Fig. 4. (continued).**

PP test results, the KPSS test fails to reject the null hypothesis of stationarity. Thus, all the variables used in the empirical analysis are stationary in nature.

4. Methodological approach

The wavelet-based analysis processes signal by taking reference from Fourier analysis and filtering methods. However, wavelets overcome the majority of the limitation of these methods (Percival and Mofjeld, 1997; Percival and Walden, 2000). One of the prime advantages of wavelets

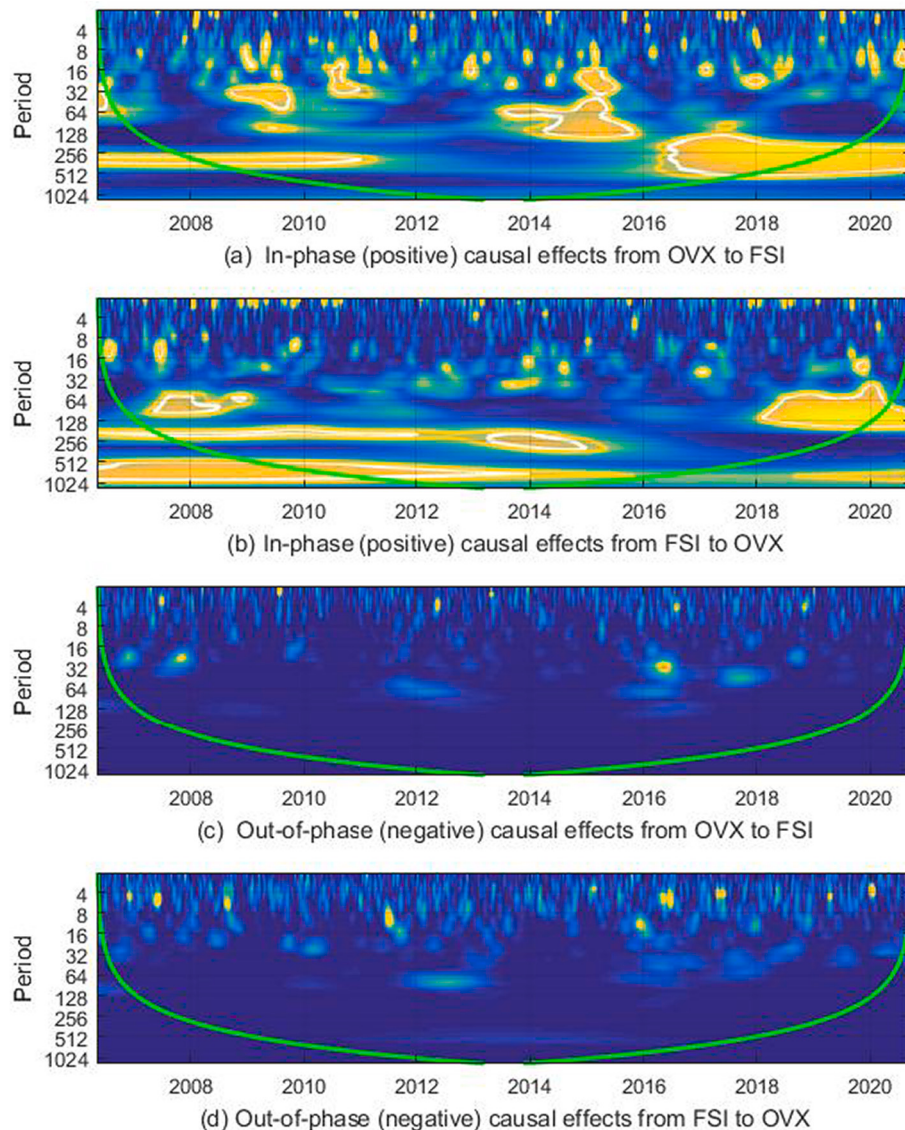


Fig. 5. a. In-phase and out-of-phase plots of causality between OVX and FSI.

- b. In-phase and out-of-phase plots of causality between OVX and Credit.
- c. In-phase and out-of-phase plots of causality between OVX and EV.
- d. In-phase and out-of-phase plots of causality between OVX and Funding.
- e. In-phase and out-of-phase plots of causality between OVX and SA.
- f. In-phase and out-of-phase plots of causality between OVX and Volatility.

Note: The *White* and *Yellow* contours in sub-figures (a) and (b) represent the statistical significance at 5% and 10%, respectively. The significance levels are derived on 3000 Monte-Carlo simulation draws estimated on ARMA (1,1) null of no statistical significance. The COI is depicted by the *green line*, which demarcates the zones affected by edge effects. The scale has been transformed to a period for the Morlet wavelet function. Using $\omega_0 = 6$ for the optimal balance (Torrence and Compo, 1998), we have $Ft = 1.033$ s.

that it conveys information in both the time and frequency domain. In addition, it relaxes any requirement of rigid assumptions concerning the data-generating process of the underlying series. The superior ability of wavelets to continuously resize its window makes it more useful and interesting. While the finer features of the data can be observed by processing the signal at a smaller window, whereas the coarse features are detected with the signal at a larger window (Torrence and Compo, 1998). In other words, short-term (long-term) dynamics of the data is

observed considering at high-frequency (low-frequency) components. Thus, the lower scales determine the short-term OVX-FSI association, by contrast the long-term association is denoted at higher scales.

4.1. Continuous wavelet framework

This study uses a continuous wavelet transformation (CWT) framework to analyse the OVX-FSI association in time-frequency domain. The

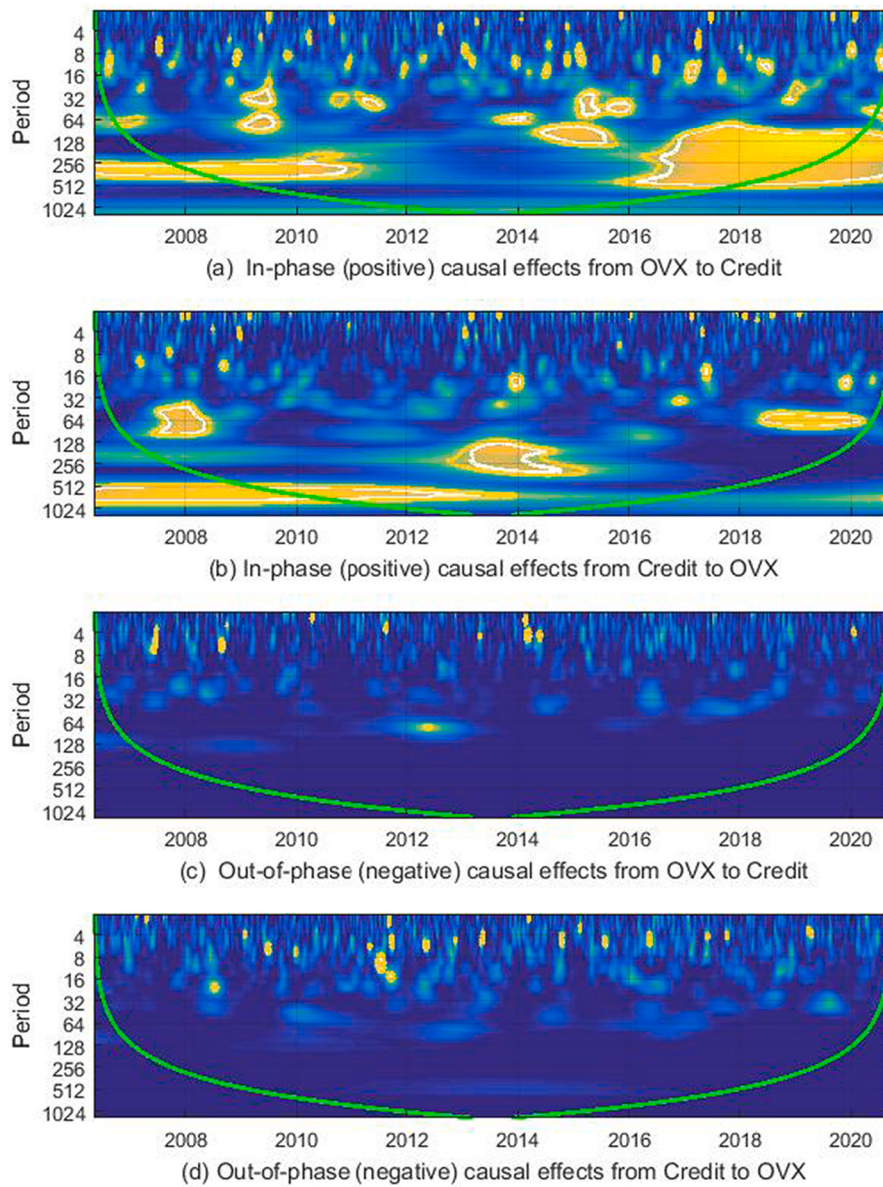


Fig. 5. (continued).

underlying data is decomposed up to level 10.³ The term *Wavelet* is a technical nomenclature referring to a ‘small wave’.⁴ The functions of wavelet are constructed depending on scale and location parameters in addition to a mother wavelet function⁵:

³ Level 1 (D1) represents 2–4 days, D2 from 4 to 8 days, D3 from 8 to 16 days, D4 from 16 to 32 days, D5 from 32 to 64 days, D6 from 64 to 128 days, D7 from 128 to 256 days, D8 from 256 to 512 days, D9 from 512 to 1024 days, D10 >1024 days (up to 2.81 years), considering civil year. The representation of scales follow Madaleno and Pinho (2014).

⁴ It is attributed as *small* because the function of wavelet is compactly supported (non-zero over a finite length of time). Further, the function is oscillatory, hence referred as *wave*.

⁵ The mother wavelet function is denoted by $\phi(t)$ and it is defined on the real-axis. It must satisfy the following conditions: (a) $\int_{-\infty}^{+\infty} \phi(t) dt = 0$ and (b) $\int_{-\infty}^{+\infty} |\phi(t)|^2 dt = 1$. These conditions potentially imply that at the least some coefficients derived of the wavelet function must stand different from zero. Further, these departures from zero must cancel out.

$$W_{s,t} = \frac{1}{\sqrt{s}} \phi\left(\frac{t-\tau}{s}\right) \quad (1)$$

Put it differently, the CWT with respect to wavelet ϕ , is essentially a function $W_x(s, \tau)$, which is mathematically expressed as:

$$W_x(s, \tau) = \int_{-\infty}^{+\infty} x(t) \frac{1}{\sqrt{s}} \phi^*\left(\frac{t-\tau}{s}\right) dt \quad (2)$$

where, the complex conjugate form is denoted by *. In order to generate the other window function, the mother wavelet $\phi(t)$ assists as a prototype. The location of the window that indicates the position of the wavelet is given by the translation parameter, τ . The embedded information regarding time in the transform domain is obtained as the window shifts through the signal. The checks on the length of the wavelet i.e., the dilation (if $|s| > 1$) or the compression (if $|s| < 1$), is given by the scaling parameter s . The wavelet transformation W_x , will be complex if the corresponding wavelet function $\phi(t)$ is complex. To disentangle the frequency-based information, dilation or compression of the mother

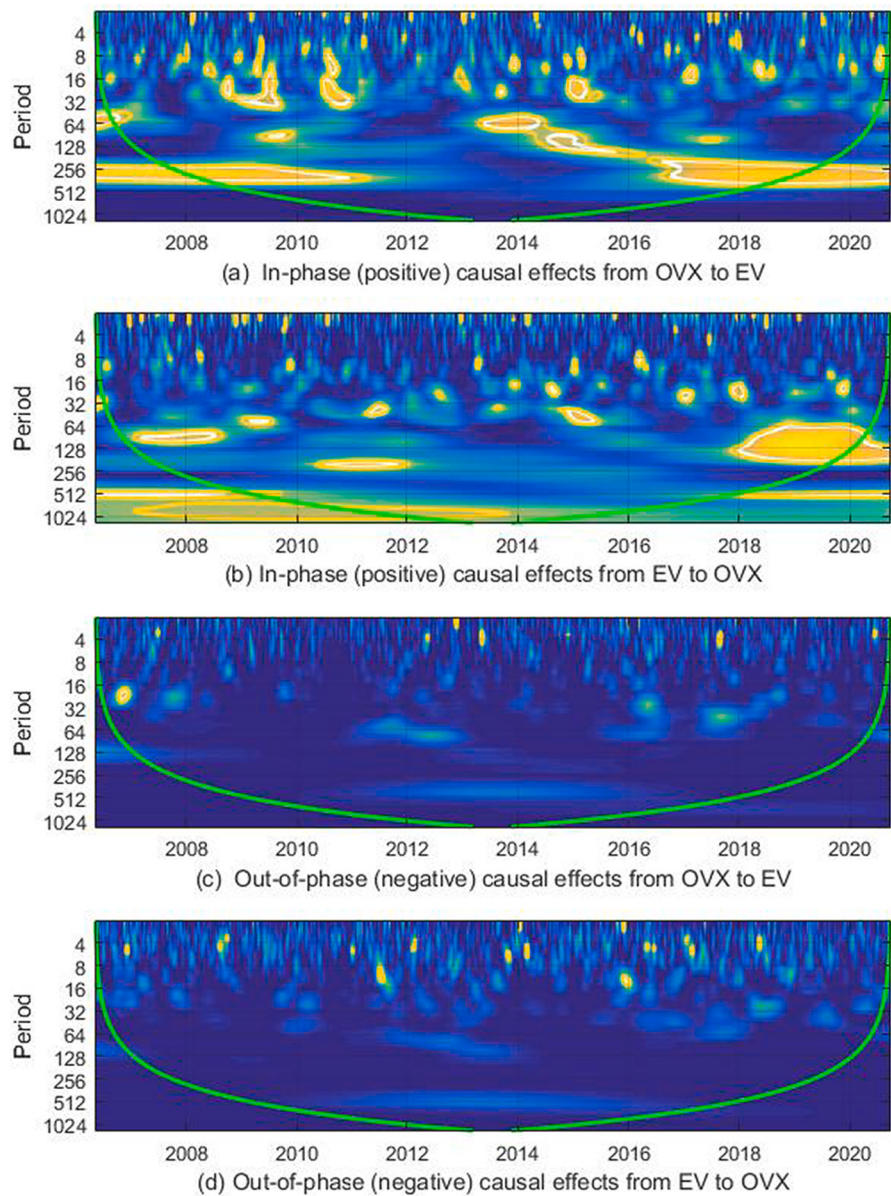


Fig. 5. (continued).

wavelet correspond to the cycles of different frequencies. However, the extent to which the mother wavelet is dilated or compressed depends on the scaling parameter s . The wavelets constructed over the horizon of short timescales tend to incorporate sharp and high-frequency volatility. The shorter timescales ensure better time resolution, however, poorer scale resolution. By contrast, the wavelets structured over long-scales tend to integrate low-frequency volatility. Hence, they have relatively poorer time resolution and better scale resolution. Furthermore, wavelet transformations can be used where the time series contain non-stationary power at various intervals (Percival and Walden, 2000). The coefficients of wavelet transformation $W_x(s, \tau)$, engulf both analysing wavelet $\phi(t)$ and the function $x(t)$. The choice of wavelet for the purpose of analysis is a significant consideration (Percival and Walden, 2000). This study uses the 'Morlet' wavelet as a basis for wavelet

transformation given its rich applicability in the areas of economics and finance (Das et al., 2018a; Das and Kumar, 2018; Madaleno and Pinho, 2014).

4.2. The Morlet wavelet; power spectrum; cross-wavelet and coherence

Proper isolation of periodic signals and a good identification is allowed by the Morlet wavelet, as it strikes an optimum balance between time and frequency-localization. This is a form of complex wavelet transformation with information on both phase and amplitude, which is essential to decipher the synchronous behaviour between time series (Aguiar-Conraria et al., 2008; Torrence and Compo, 1998). The central frequency of the Morlet wavelet for analysing the data is set to ten ($W_0 = 10$). Thus, the special characteristics of the signals can be estimated as

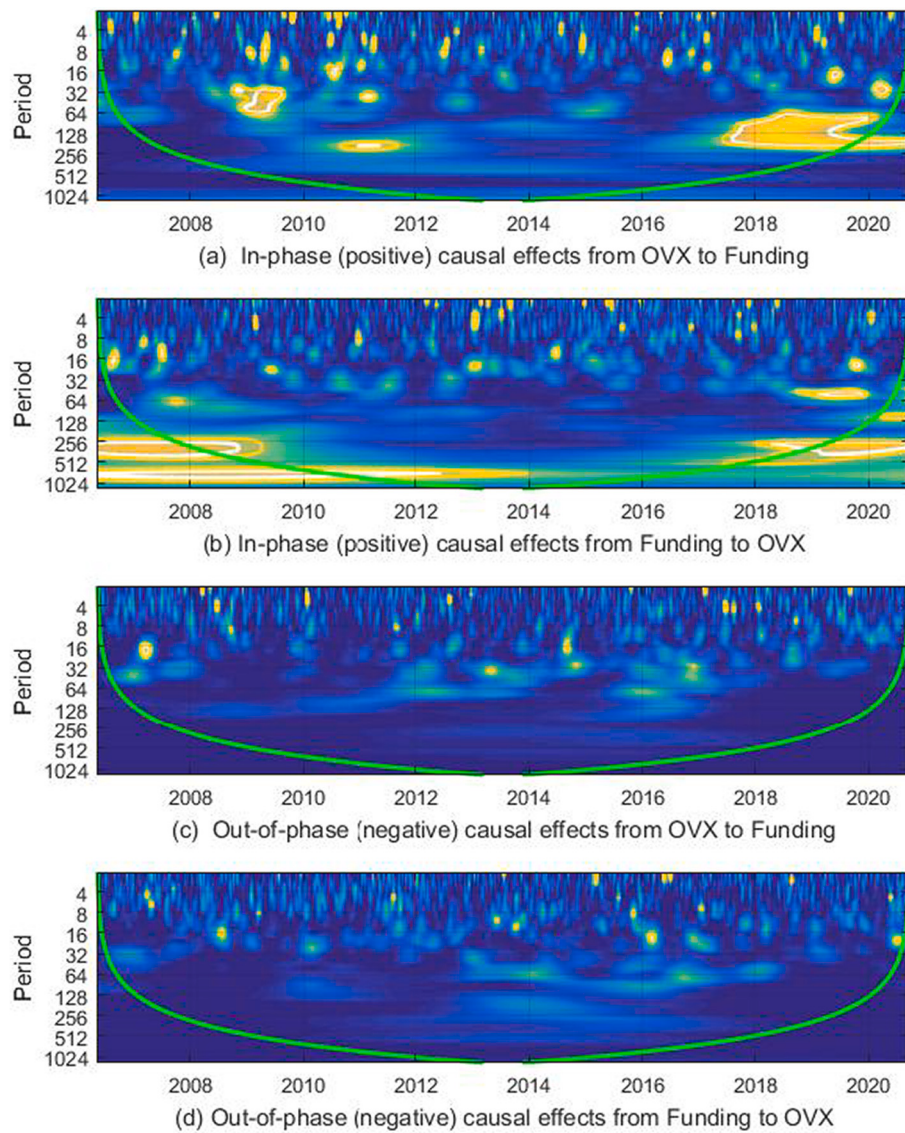


Fig. 5. (continued).

a function of time. In addition, the wavelet-based analysis not only provide the time-varying power spectrum, but for the computation of coherence phase spectrum is also required.

The association between two time series is expressed by correlation, so that one can affirm the highly correlated series as coherent.⁶ The measure of how two variables x and y are associated by a linear transformation is expressed by the degree of coherence. If the degree of coherence between a set of variables is tending to the maximum value of unity, only then the variable set may be related closely in a linear transformation. Thus, a pair of random variables is assumed to be coherent if and only if $|\rho| = 1$, and incoherent if and only if $|\rho| = 0$, where the correlation coefficient is given by ρ . Nevertheless, it is essential to note that the correlation may not be contemporaneous in all

the cases. It may also involve a lead-lag behaviour. Phases are used to determine the magnitude of lead or lag characteristics.

While considering discrete underlying time series $\{x_n, n = 0, \dots, N - 1\}$ of observation N featuring a uniform time step δt , the integral expression in eq. (14) is to be discretized, hence the CWT of time series $\{x_n\}$ is revised as:

$$W_m^x(s) = \frac{\delta t}{\sqrt{s}} \sum_{n=0}^{N-1} x_n \phi^* \left((n-m) \frac{\delta t}{s} \right), m = 0, 1, \dots, N-1 \quad (3)$$

Suffering from the border distortions is inevitable while applying the CWT to a time series of finite length. The primary cause being the values of the transform are always imprecisely computed at the end and the beginning of the series. It encompasses missing values of the series which are then set synthetically. Further, it is important to note that the effective support of the wavelet at scale s stands proportional to s , hence the edge effects also enhance with s . The area in which the transformation is plagued by those edge effects are referred as the cone of influence. This region falls beyond the statistical significance and hence must be interpreted carefully (Torrence and Compo, 1998).

The wavelet power spectrum (WPS) is denoted by $|W_n^x|^2$. WPS typically exemplifies the spectral density (distribution of energy) of a designated time series in the time-scale plane. The cross-wavelet

⁶ The coherence is often considered equivalent to the measure of correlation. However, there exist some differences between them. In the computation of coherence, the signal is squared and thus it produces value ranging from 0 to 1. In this case the information related to polarity is lost. In contrast, the correlation is polarity-sensitive and its value ranges typically from -1 to 1 . Hence, coherence unearths information pertaining to the stability of relationship between two signals with respect to phase relationship and power asymmetry.

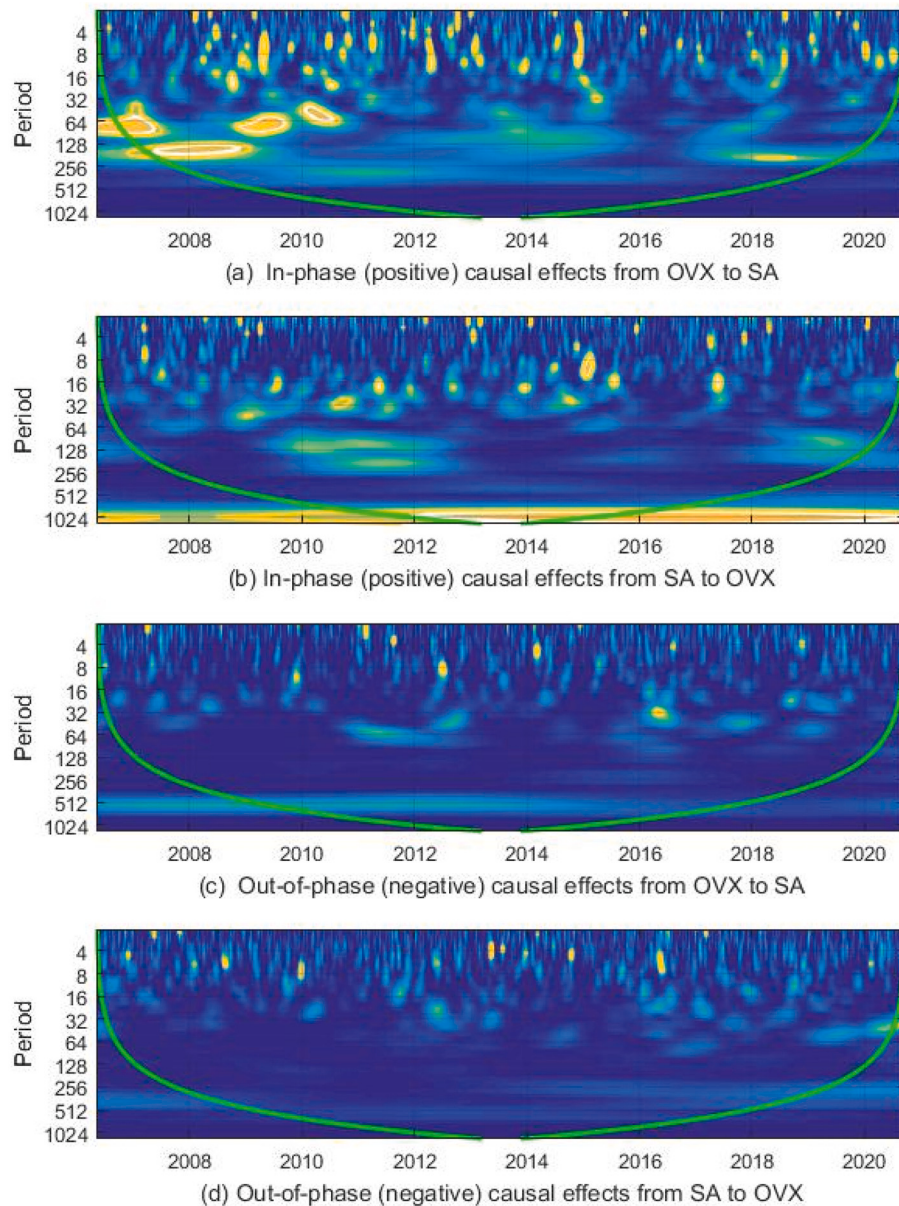


Fig. 5. (continued).

transform (XWT) of a pair of time series x_n and y_n is defined as $W_n^{xy} = W_n^x W_n^{y*}$, where the complex conjugate is denoted by $*$, and the wavelet transformation of the series x_n and y_n is given by W_n^x and W_n^y , respectively. While the WPS exhibit the local variance of a single time series, the XWT depicts co-variance of the pair of time series at each frequency or scale. Any lead or lag relationship between the components are identified by phases of the wavelet, which is defined as:

$$\phi_{x,y} = \tan^{-1} \frac{I\{W_n^{xy}\}}{R\{W_n^{xy}\}}, \phi_{x,y} \in [-\pi, \pi] \quad (4)$$

where the real and imaginary parts of the smooth power spectrum are denoted by I and R , respectively. The phase relationship between two variables can be characterized by phase differences. In the coherence map, the phase differences are indicated by arrows. Whether the time series are in-phase or anti-phase, are indicated by left-tailed (\rightarrow) or right-tailed (\leftarrow) arrows, respectively. In-phase time series depict positive co-movement, whereas the anti-phase behaviour denote negative co-movement. The arrows pointed upwards (\uparrow), right-upward (\nearrow) and

left-downward (\swarrow) indicate the first time series is leading the second. Similarly, the downward (\downarrow), right-downward (\searrow) and left-upward (\nwarrow) pointed arrows show the second time series tend to lead of the first.

The wavelet-based coherency of a pair of time series, following Torrence and Compo (1998), may be defined as:

$$R_n^2(s) = \frac{|S(s^{-1}W_n^{xy}(s))|^2}{S(s^{-1}|W_n^x(s)|^2) \cdot S(s^{-1}|W_n^y(s)|^2)} \quad (5)$$

where the smoothing operator in both time and scale is represented by S . The definition closely characterizes the traditional connotation of a correlation coefficient. The wavelet coherence may be thought as localized correlation in frequency space. The XWT coherence indicates coherence between the rotary components. The coherency of 1 denote stronger co-movement indicated by hot red zones on the coherence maps. Lower coherency of (or tending to) 0 denote weaker co-movement, indicated by cold blue zones. In other words, the local correlation between CWT can be defined as the cross-spectrum ratio to the product of the spectrum of each series.

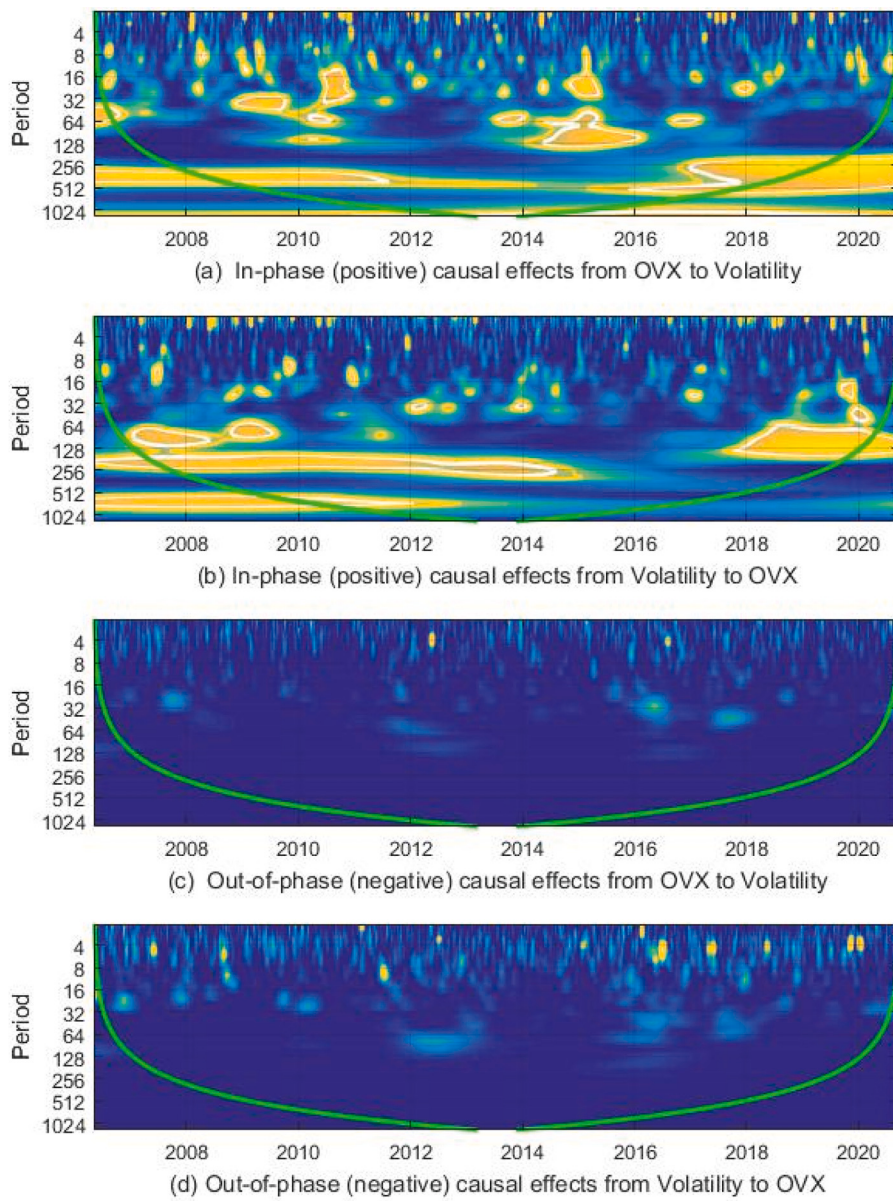


Fig. 5. (continued).

4.3. Causality in continuous wavelet transformation

The conceptualization of causal association between a pair of variables is perhaps one of the well-appreciated econometric ideas. The traditional method to estimate causality such as the Granger causality approach (Granger, 1969) has a rich applicability in the areas of economics and finance beside others. One of the shortcomings of this method pertains to its inability to distinguish the causality in the long-run from causality in the short-run. To address this issue, Geweke (1982) conceived the idea of detecting causality in the frequency domain, which is deliberated by subsequent scholars. Later, Olayeni (2016)⁷ proposes Granger-causality in a CWT framework that depends upon the wavelet-based correlation measure of Rua (2013), which is given by:

$$G_{Y \rightarrow X}(s, \tau) = \frac{\zeta\{s^{-1}|R(W_{XY}^m(s, \tau))I_{Y \rightarrow X}(s, \tau)|\}}{\zeta\left\{s^{-1}\sqrt{|W_X^m(s, \tau)|^2}\right\} \cdot \zeta\left\{s^{-1}\sqrt{|W_Y^m(s, \tau)|^2}\right\}} \quad (6)$$

where, the wavelet-based transformations are given by $W_X^m(s, \tau)$, $W_Y^m(s, \tau)$ and $W_{XY}^m(s, \tau)$. The indicator function is given by $I_{Y \rightarrow X}(s, \tau)$, which is defined by Olayeni (2016) as:

$$I_{Y \rightarrow X}(s, \tau) = \begin{cases} 1, & \text{if } \phi_{x,y}(s, \tau) \in \left(0, \frac{\pi}{2}\right) \cup \left(-\pi, \frac{\pi}{2}\right); \\ 0, & \text{otherwise} \end{cases} \quad (7)$$

This method is supposedly useful in the case of this paper as it can detect bidirectional causality between OVX and stress indexes in a time-frequency domain. Further, this method is also useful to detect causalities during the periods of high and low oil volatility and financial stress. Several studies in the past use this methodological approach in the context of energy, equity and metals market to detect causality in CWT framework (for instance, Alam et al., 2019; Kang et al., 2019; Tiwari

⁷ The methodological modification suggested by Olayeni (2016) is described briefly. The interested readers are requested to refer Olayeni (2016) for a detailed discussion on evolution of spectral causality techniques.

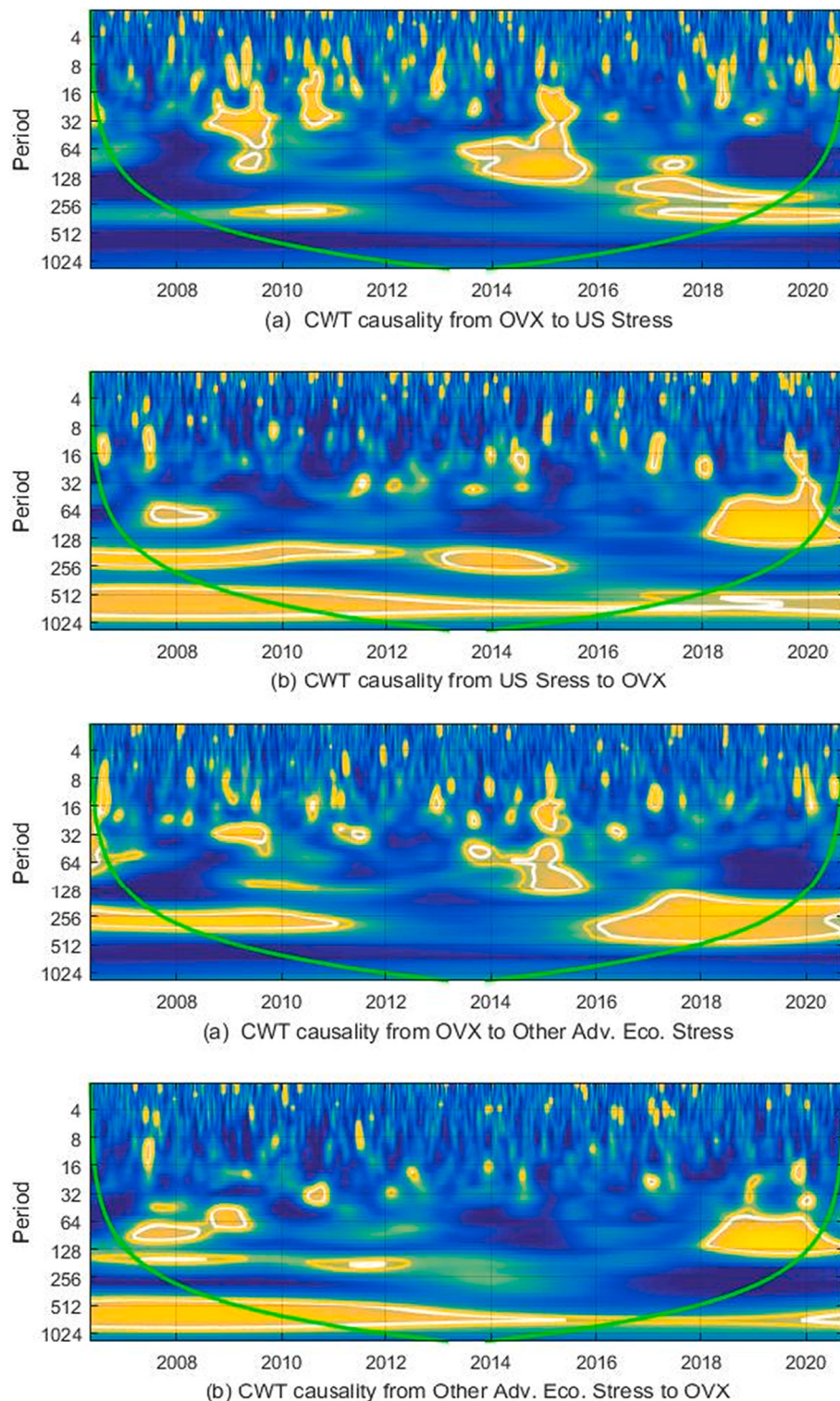


Fig. 6. a Continuous wavelet transform plot of causality between OVX and US stress.

b. Continuous wavelet transform plot of causality between OVX and Other Advanced Economies stress.

c. Continuous wavelet transform plot of causality between OVX and Emerging Market stress.

Note: The *White* and *Yellow* contours in sub-figures (a) and (b) represent the statistical significance at 5% and 10%, respectively. The significance levels are derived on 3000 Monte-Carlo simulation draws estimated on ARMA (1,1) null of no statistical significance. The COI is depicted by the *green* line, which demarcates the zones affected by edge effects. The scale has been transformed to a period for the Morlet wavelet function. Using $\omega_0 = 6$ for the optimal balance (Torrence and Compo, 1998), we have $Ft = 1.033$ s.

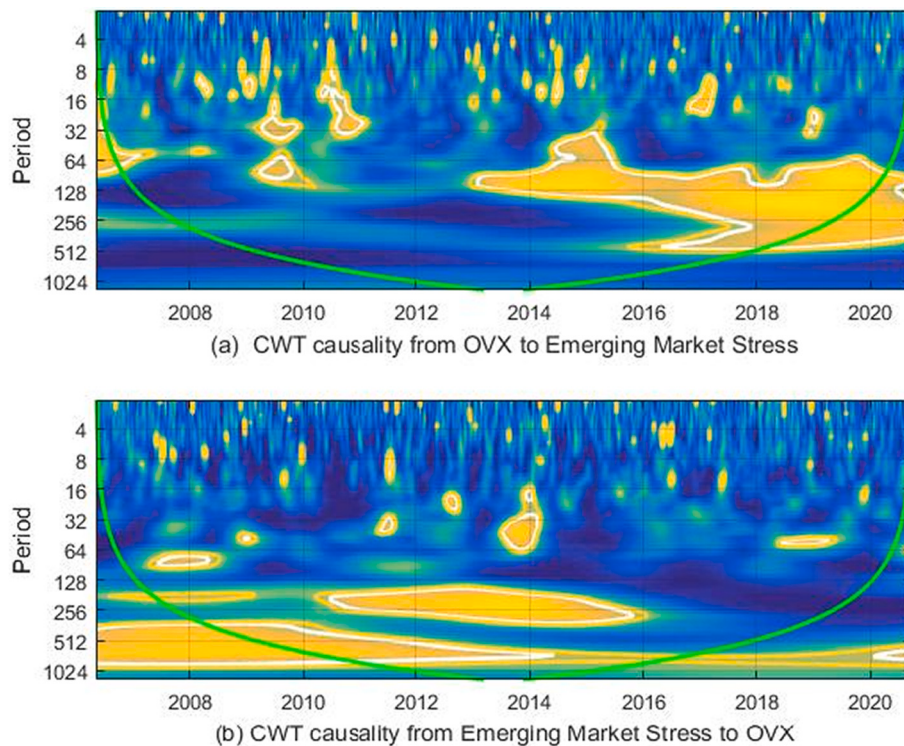


Fig. 6. (continued).

et al., 2018a; Tiwari and Albulescu, 2016).⁸

5. Empirical results

This section discusses the results and explains their implications under the light of economic theories. First, the results obtained from VAR Granger-causality approach is reported in Table 6. The VAR Granger-causality test follows the modified Wald (MWALD) statistics to examine Granger non-causality as the null hypothesis (H_0). The MWALD statistics follow a chi-square (χ^2) distribution with k degrees of freedom. The results show that the null of non-causality can be rejected in most of the cases. Further, the evidence of bidirectional causality is also prominent as affirmed in the previous literature (Das et al., 2018b; Nazlioglu et al., 2015). The null of non-causality is accepted in the case of OVX→SA, SA←OVX and OVX→Funding pairs. The stress concerning SA denote the valuation measures of the asset class which has a stable cash flow in general. It is true that the assets that constitute the SA index such as gold and bonds could co-move with equity markets during the phases of economic turbulence, it remains tranquil during normal periods, nonetheless. Baur and Lucey (2010) find that gold remain uncorrelated with the mainstream financial assets during normal periods, however, during the stressed periods gold becomes correlated shortly as investors fly to safety. Thus, insignificant flow of causality between oil uncertainty and SA stress for the full sample seems unsurprising. In the context of OVX→Funding, the non-causality is somewhat surprising. Theoretically, economic uncertainties pronounced by OVX is expected to enhance the

risk premium and cost of borrowing resulting in higher probabilities of default for the firms and eventually the propensity to invest is curbed (Apostolakis et al., 2021). One plausible reason could be that the underlying indexes used to construct the Funding stress index have not been impacted much by OVX.

Next, the results for WPS are discussed for all the variables, as presented in Fig. 2. While the horizontal axis of the WPS maps indicates the timeline, the vertical axis denotes the frequencies converted in terms of days for ease of interpretation. The strength of the spectral density is indicated by the colour bar ranging from low to high, indicated by blue to red, respectively. The funnel-shaped curve denotes the cone-of-influence (COI) the area below the curve indicates the zones affected by edge effects. The black bounded contours on the map highlight the regions that are significant at 5% level estimated using the Monte Carlo simulations. It is interesting to note that in the case of OVX, significant zones with power conservation are limited during GFC 2007–08. Nevertheless, significant zones are identifiable around the period of COVID-19 up to ~256 days. It essentially emphasizes that the crude oil markets were less affected by economic shocks during 2007–08 than COVID-19. This result seems justifiable as a major travel and industrial restrictions were posed worldwide during COVID-19. In the context of composite FSI and categorical stress indexes, significant power zones are identifiable for GFC 2007–08 and COVID-19 up to and over ~256 days. Notably, the exposure of stress indexes seems higher during 2007–08 since it was a crisis of financial nature. Further, it is also interesting to note that the impacts of COVID-19 on the SA and Funding markets are marginal. Nonetheless, the historical evolution of all the variables depicts some common feature which is investigated further.

Fig. 3 presents the result of the Wavelet Coherence Analysis (WCA) between OVX and the composite and categorical stress indexes. The figures show that the dependence between OVX and stress indexes are time and frequency-varying over the window of the study. The horizontal axis defines the sphere of time, whereas the vertical axis indicates the frequencies in terms of the number of days. The bold black contours on the surface of coherence maps indicate significant local correlations at 5% level and are estimated using the Monte Carlo simulations. The

⁸ In order to examine causality in the wavelet framework few studies in the past use Discrete Wavelet Transformation (DWT) and then use the Granger-causality (for instance, see Jiang and Yoon, 2020; Reboredo et al., 2017; Tiwari et al., 2013). Olayeni (2016) argues that this approach fails to capture the causal effects in time-domain and hence it is as good as the Granger-Geweke measure of causality only in the frequency-domain. Thus, Olayeni (2016) suggests the current method as it circumvents the limitations of using the blended DWT-Granger causality model.

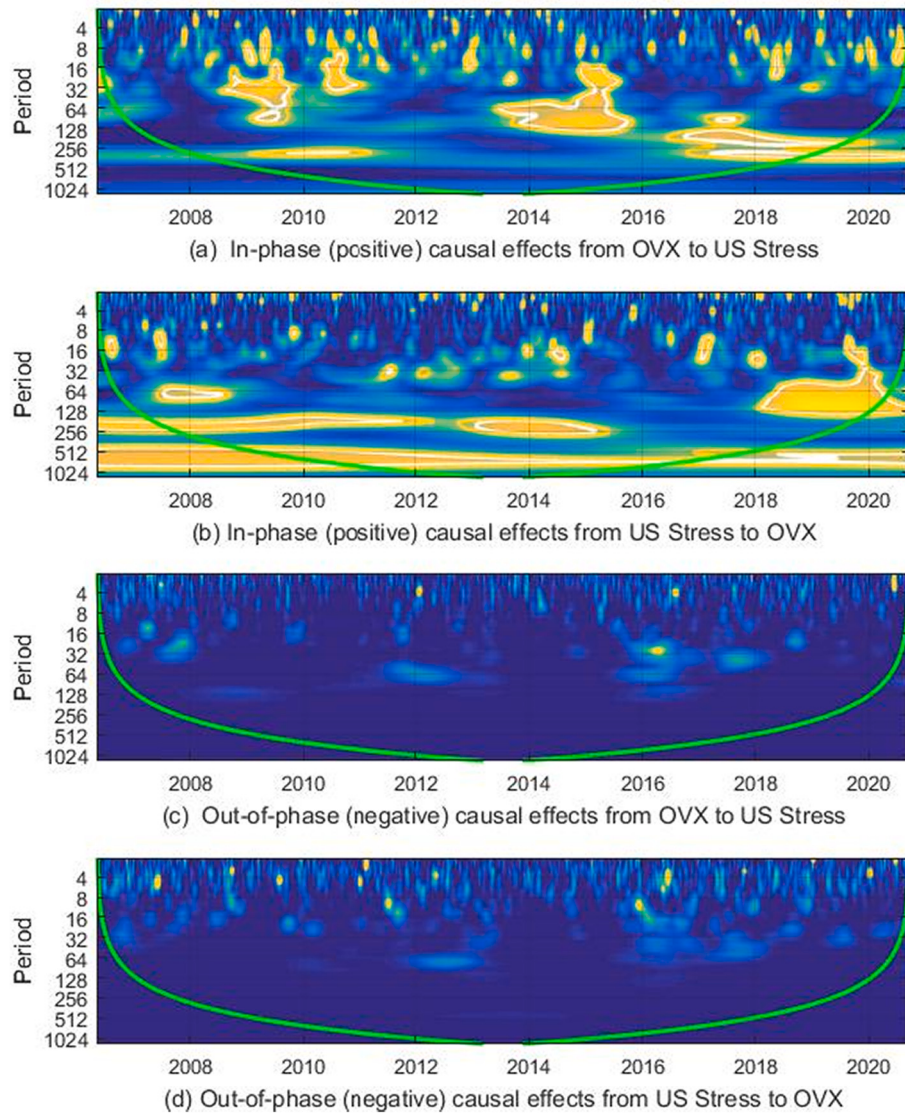


Fig. 7. a. In-phase and out-of-phase plots of causality between OVX and US stress.
 b. In-phase and out-of-phase plots of causality between OVX and Other Advanced Economies stress.
 c. In-phase and out-of-phase plots of causality between OVX and Emerging Markets stress.

black funnel-shaped line, which demarcates the zones affected by edge effects, is the COI. The stronger (weaker) coherencies are depicted by the red (blue) zones as designated by the colour bar. Further, the arrows on the surface of the coherence maps indicate the phases. The positive co-movements are indicated by right-pointed (\rightarrow) arrows, while the negative association is ascribed by left-pointed (\leftarrow) arrows. The lead-lag dynamics among a pair of variables is expressed by the arrows pointed upwards (\uparrow), right-upward (\nearrow) and left-downward (\swarrow), which indicates the first time series is leading the second. Similarly, the downward (\downarrow), right-downward (\searrow), and left-upward (\nwarrow) pointed arrows show that the second time series tend to lead to the first. Throughout the analysis, OVX is considered as the first series, while the stress-related indexes represent the second series. Fig. 3a exhibits the wavelet coherency between OVX and composite FSI, revealing certain interesting characteristics about the OVX-FSI association. Though some small and discrete, black-bounded contours are visible at high frequency, however, the overall dependency is weak. Relatively higher continuous and coherent dependency is observed in the medium to low frequencies starting from ~ 32 days. It is noteworthy that higher and long-run coherencies are concentrated around the period corresponding to the crisis period. The

coherence persists until the post-crisis period, i.e., mid-2011, at lower frequencies of ~ 256 days and above. The coherence, however, decays subsequently as the crisis condition tranquillizes. Another discrete significant coherence island is observable between ~ 32 – 128 days around the period 2014–16. This period is associated with higher volatilities in the oil market due to oil oversupply shocks (Dutta, 2018). Another black-bounded and significant zone is cognisable around the period of COVID-19 in the frequency of ~ 16 to 256 days. Regarding the direction of the relationship, the coherence maps are largely dominated by rightward pointed (\rightarrow) arrows indicating positive association. In terms of the lead-lag relationship, the results are not very convincing to interpret. Nevertheless, after the 2007–08 crisis, around frequencies ~ 256 days and above, some right-downward (\searrow) arrows are dominant. It indicates that the volatility in oil markets tends to follow financial conditions. In other words, the financial market stress is transmitted to the oil markets. The underlying reason could be manifold, such as the contagion mechanism or the financialization of oil beyond others (Bianchi et al., 2020; Madaleno and Pinho, 2014). Similarly, during the phase of COVID-19, around ~ 32 – 64 days, some right-upward (\nearrow) arrows are perceivable, meaning the financial stress trailed the volatility in the oil market.

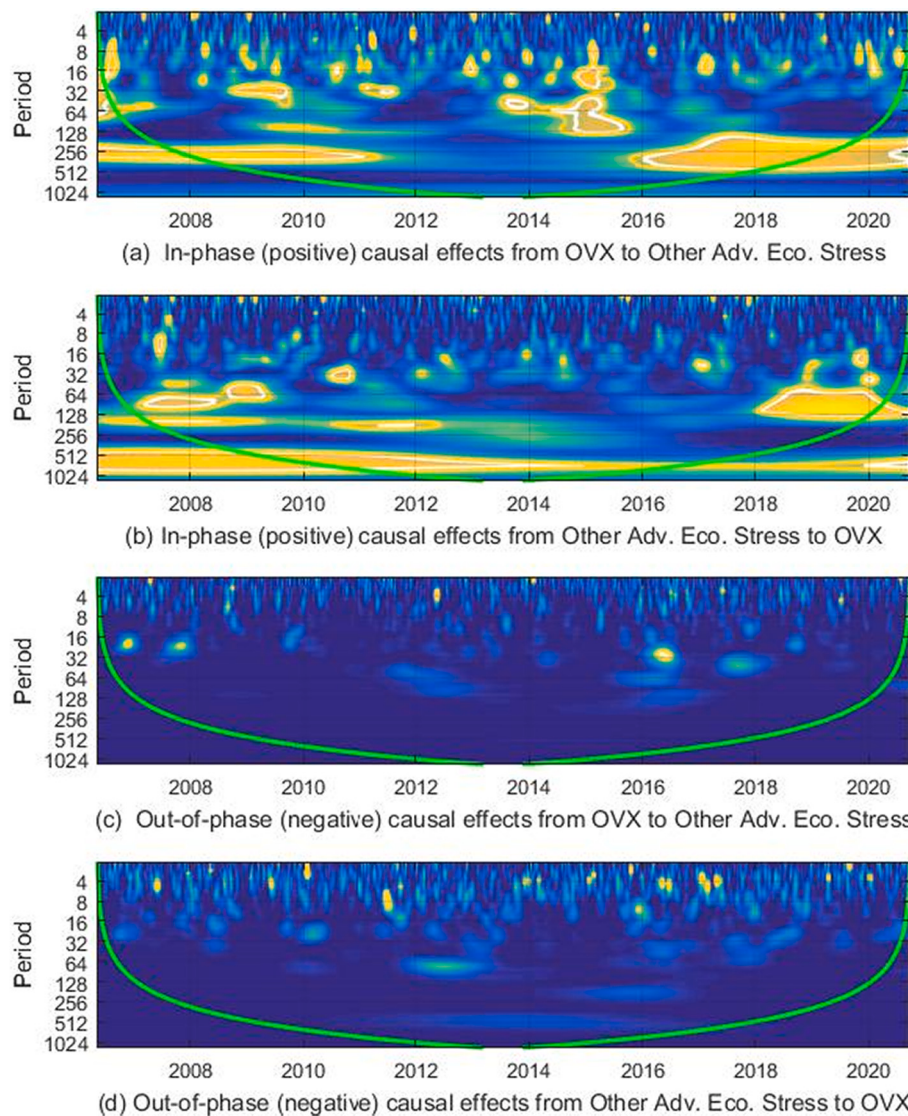


Fig. 7. (continued).

It is imperative to understand the similarities (or differences) in the co-movement dynamics of the categorical stress indicators compared to composite FSI with respect to OVX. The case of credit-related stress represents the difference in borrowing costs for firms of different creditworthiness. Higher oil volatilities could impede economic activities affecting credit markets and banking systems adversely. On the other side, the conditions of financial stress forerun lower energy demands due to shrinkage in the public investments (Nazlioglu et al., 2015). During turbulent times the distress risks are bound to enhance due to increased risks in the macroeconomic environment and a fall in consumer demands. Thus, a firm may decide to produce in concurrence with revised demands leading to lower energy consumption. Fig. 3b depicts the association between credit and OVX in the time-frequency space. The overall findings are somewhat consistent with the results of the composite FSI. Three major islands of significance are observable around GFC (2007 onwards), oversupply shock (around 2014–16) and COVID-19. Further, the arrows indicate positive relationship between credit stress and OVX. The lead-lag relationship is marginally identifiable, for instance, around 2019–20 at frequencies ~128–256 days some right-downward (\searrow) arrows are evident. The causal forces that stimulate the lagged behaviour in the oil volatility could stem from the shocks in the credit markets as public investment and energy demands diminish.

Fig. 3c exhibits the coherencies between OVX and equity valuation.

The valuation of equities reflects the confidence of investors in the real economy and their risk appetite. The co-movement behaviour between OVX and equity valuation-related stress is somewhat consistent with composite FSI and credit stress. Nonetheless, the arrows depict a persistent positive relationship. Further, during the initial phases of COVID-19 i.e., around 2020 a few right-upward (\nearrow) arrows suggest stress in equity valuation follows OVX as consistent with previous literature on oil and equity relationship (Das and Kannadhasan, 2020; Xiao et al., 2019). Fig. 3d denotes the coherencies between OVX and funding related stress. The funding stress seems to co-move significantly during GFC and COVID-19. During GFC, the phases expressed by arrows are pointed upwards (\uparrow) and right-upward (\nearrow) meaning OVX leads the stress in funding markets. The previous literature establishes the influential role of impending oil shocks on currencies and interest rates (Ioannidis and Ka, 2018; Kunkler and MacDonald, 2019). Further, during COVID-19 strong and persistent positive association is observed between the pair of variables as expressed by rightward pointed (\rightarrow) arrows.

Fig. 3e shows the coherencies between OVX and stress in safe assets. Safe assets are securities with stable and predictable cash flows and are preferred by investors during the phases of an economic downturn. The coherencies of OVX are minimal with respect to stress in safe assets. The coherencies are mainly observable around GFC and during the phase of

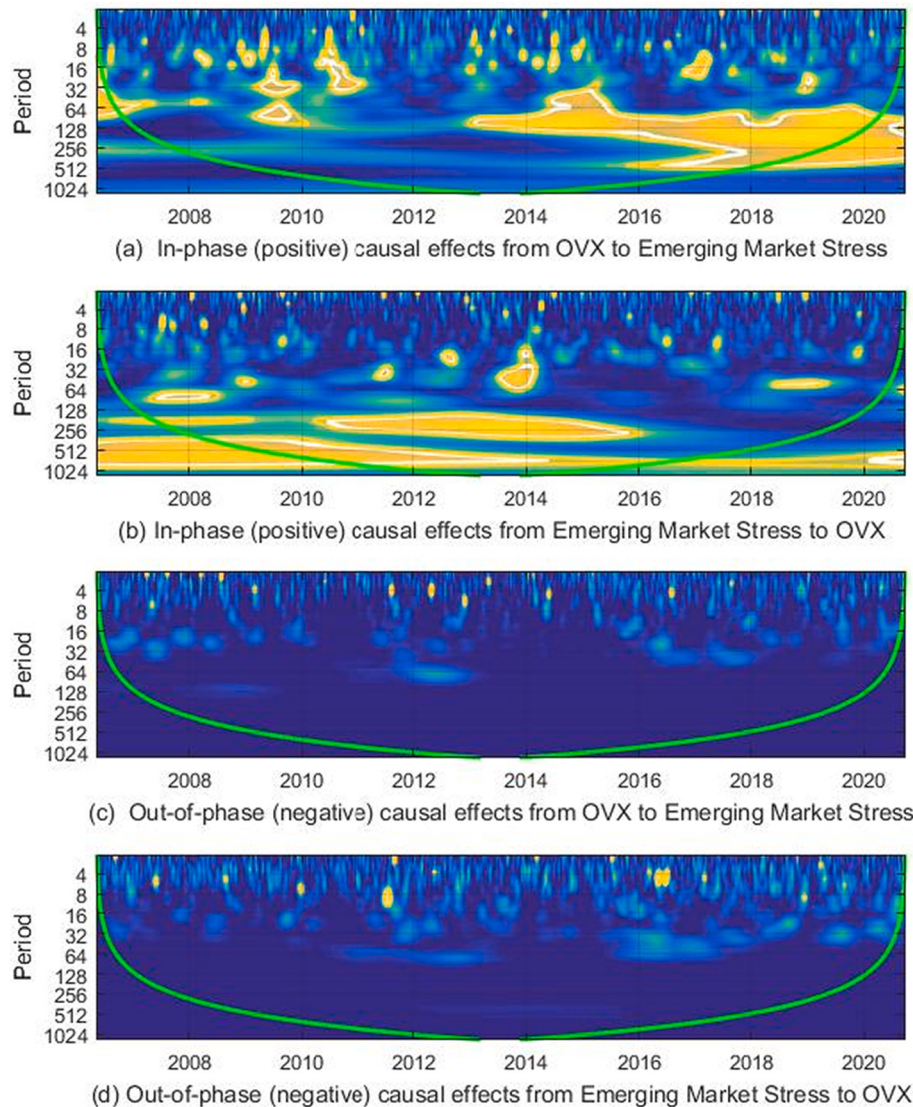


Fig. 7. (continued).

oil oversupply shock in 2014–16. Surprisingly, negligible coherencies are observed around the phase of COVID-19. Regarding phases, right-downward (\searrow) arrows dominate the maps around the aforementioned crisis periods. Investor's precautionary flight to safety ahead of the fluctuations in oil markets could be a plausible reason for OVX to the trail. Lastly, Fig. 3f presents the co-movement of OVX with volatilities of equity, credit, currency, and commodity markets. The coherencies are persistent over ~ 32 days across all the major macroeconomic events. The phases indicate a strong positive association, and volatility stress follows OVX $\sim 32\text{--}256$ day's frequency around GFC in 2009. This finding is consistent with prior literature establishing the association between OVX and implied/realized volatilities of equity and commodity markets (Dutta, 2018; Maghyereh et al., 2016; Xiao et al., 2019).

Though the traditional wavelet coherence analysis reveals only the co-movement dynamics between a pair of variables in the time-frequency domain, it remains silent on the causality between the variables. To overcome this issue and draw inferences on the causal association between the variables in the time-frequency domain, the causal wavelet approach proposed by Olayeni (2016) is used. Fig. 4a-f exhibit the continuous wavelet transform plots of pairwise directional causalities between OVX and stress indexes in sub-figures (a) and (b). Within the maps, the white and yellow contours represent the statistical

significance at 5% and 10%, respectively. The yellow zones denote spheres of high causality, whereas the blue zones indicate lower or no causality.

Withstanding the results of the wavelet coherence analysis, the wavelet-based causalities also appear episodic around the periods of economic turbulence. Fig. 4a presents the continuous causalities between OVX and composite FSI in pairs sub-figure (a) depicts the causalities transmitted from OVX to FSI. In contrast, the reverse causality is exhibited by sub-figure (b). It is apparent that continuous and significant zones of causalities running from OVX to FSI exist mainly around the aforementioned periods of crisis for frequencies ~ 16 to over 256 days. Similar patterns can be observed in the reverse case. Nevertheless, it seems that causalities transmitted from OVX are stronger than otherwise. In the causality transmission between OVX and credit-related stress, as depicted in Fig. 4b, the timeline of causality is consistent with the baseline stress measure. Interestingly, the evidence that stronger transmissions are emitted from OVX towards credit stress is convincing in this case around frequencies $\sim 64\text{--}256$ days. Similar inferences can be drawn for the other stress components such as equity valuation, funding, safe assets and volatility with respect to OVX as depicted by Fig. 4c-f. In each pair, OVX appears to be the stronger emitter of causal forces. Moreover, the intensity of causal transmission is

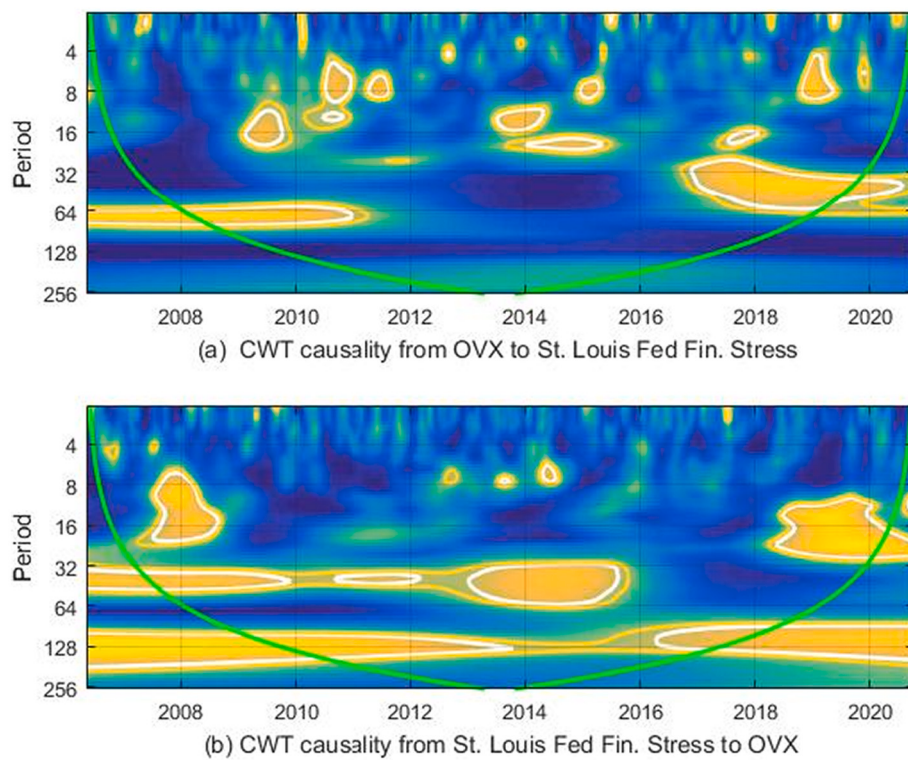


Fig. 8. Continuous wavelet transform plot of causality between OVX and St. Louis Fed Financial Stress Index.

Note: The White and Yellow contours in sub-figures (a) and (b) represent the statistical significance at 5% and 10%, respectively. The significance levels are derived on 3000 Monte-Carlo simulation draws estimated on ARMA (1,1) null of no statistical significance. The COI is depicted by the green line, which demarcates the zones affected by edge effects. The scale has been transformed to a period for the Morlet wavelet function. Using $\omega_0 = 6$ for the optimal balance (Torrence and Compo, 1998), we have $F_t = 1.033$. s.

heterogeneous across the stress components. Unsurprisingly, the transmission of causality is minimum for safe asset stress, which was also demonstrated by the wavelet coherence results. Hence, it may be inferred that causalities that exist between stress and OVX are stronger and more convincing, mainly around the phases of economic turbulences at various frequencies. Further, the strength of such causalities is time-varying and mostly emitting from OVX to stress components.

Lastly, to attest to the association between OVX and stress components further, the sample period is bifurcated into a distressed and normal state of economic affairs. Such an investigation is relevant as it may reveal the difference in predictive linkages across different economic regimes. The economic states are defined by phases derived by decomposing the variables into positive and negative values. The positive values of OVX and stress component define an economic phase of higher oil volatility and high stress, i.e., an adverse economic condition (or a distressed period). Conversely, negative values indicate a tranquil period (or a normal period).

Fig. 5a-f exhibit the results for causalities across the phases. The sub-figures (a) and (b) in the upper panels show the positive (in-phase) causalities running from OVX to stress index and vice-versa, respectively (i.e., during the distressed period). Similarly, the sub-figures (c) and (d) in the lower panels show the negative (out-of-phase) causalities in the normal periods.⁹ It is clearly evident by Fig. 5a-f that though the inferences on causal transmission remain the same, the causalities mainly exist only during the phases of adverse economic conditions. Hence, it may be concluded that the causal association between OVX and stress components are not only episodic but also becomes stronger in distressed phases.

6. OVX and financial stress across geographic regions

This section describes the causal transmissions between OVX and financial stress indexes of the geographic regions. In addition to

segment-wise stress indexes, OFR also constructs indexes for three broad geographic regions, they are: (a) the US (focussing on the US-centric variables), (b) Other Advanced Economies (encompassing variables from advanced economies other than the US, primarily focussing on Eurozone and Japan), and (c) Emerging Markets (measuring stress by focussing on the emerging market variables). Fig. 6a-c exhibit the continuous wavelet transform plots of pairwise directional causalities between OVX and stress indexes of geographic regions in sub-figures (a) and (b). In the case of the US (as depicted by Fig. 6a), islands of significance may be observed around frequencies ~8 to 128 days around the period of GFC. Similarly, as discussed earlier in the case of segment-wise stress indexes, the other islands of significance persist during the oil oversupply shock and the COVID-19 pandemic. An interesting observation is that, in this case, the causal transmission appears stronger from US stress to OVX. The plausible underlying reason could be the fact that turbulence in the US economy may influence the industrial production demand of the rest of the world by the way of economic integration (Arora and Vamvakidis, 2006; Heathcote and Perri, 2003). Nevertheless, the results for Other Advanced Economies and Emerging Markets (in Fig. 6b and c) remain consistent with the results of the segment-wise stress indexes. In both cases, OVX apparently has stronger causal influences. Interestingly OVX has the strongest influence on Emerging Market stress, which is also consistent with the recent study conducted by Das et al., 2022a. In terms of causalities across the phases, as exhibited by Fig. 7a-c, the results reinforce the fact that causal associations intensify mainly during the distressed phases.

7. Further analysis of OVX and US stress index

Lastly, further analysis is conducted to test the robustness of the findings in the case of the US stress index, which is an exception compared to all other indexes considered. In the current case, the US stress is proxied by the St. Louis Fed Financial Stress Index, which is sourced from the website of the Federal Reserve Bank of St. Louis. This data is available at a weekly frequency. The bidirectional causal association and causalities across the phases are exhibited in Figs. 8 and 9,

⁹ Other rules for interpreting the wavelet maps remain the same.

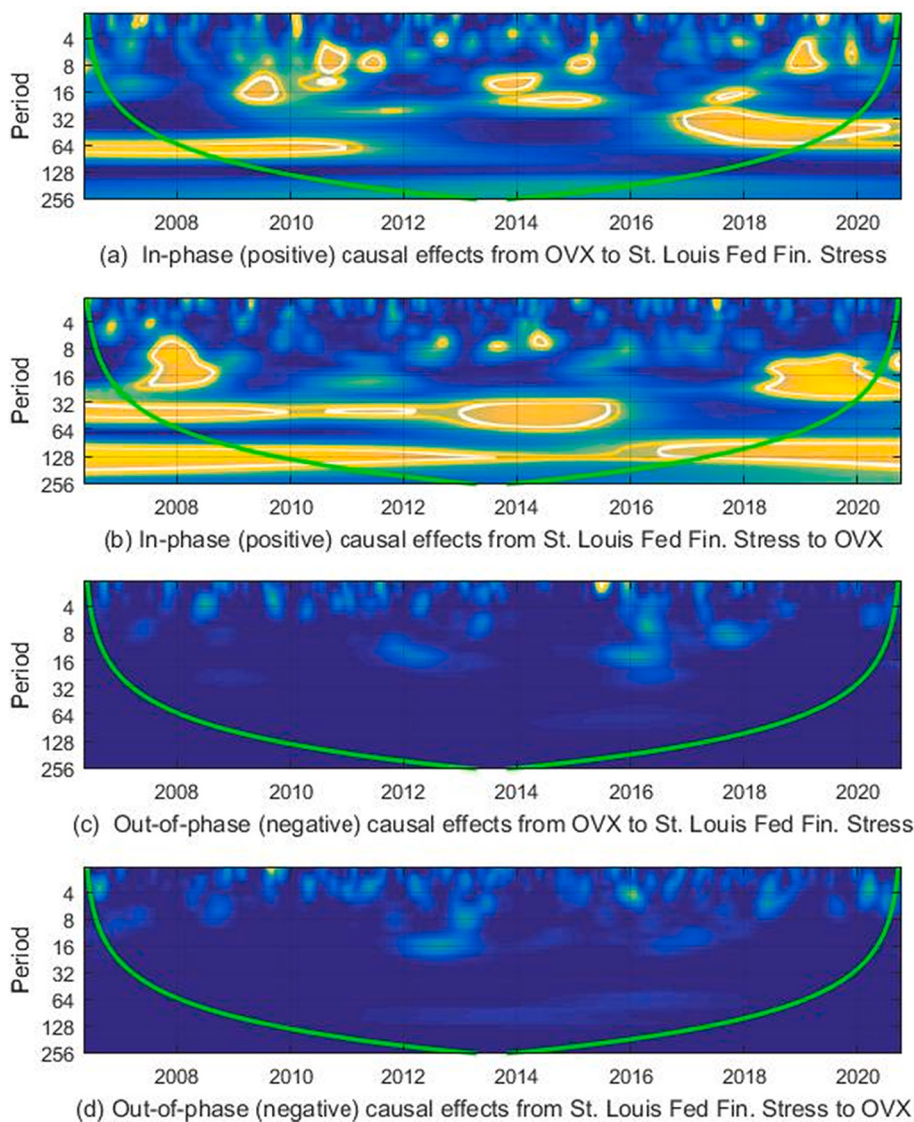


Fig. 9. In-phase and out-of-phase plots of causality between OVX and Emerging Markets stress.

Note: The White and Yellow contours in sub-figures (a) and (b) represent the statistical significance at 5% and 10%, respectively. The significance levels are derived on 3000 Monte-Carlo simulation draws estimated on ARMA (1,1) null of no statistical significance. The COI is depicted by the green line, which demarcates the zones affected by edge effects. The scale has been transformed to a period for the Morlet wavelet function. Using $\omega_0 = 6$ for the optimal balance (Torrence and Compo, 1998), we have $Ft = 1.033 \text{ s}$.

respectively. Interestingly, the baseline results remain qualitatively similar, and the stronger causal influences from US stress to OVX hold true. A detailed analysis of the factors that mediate this relationship may be the subject of detailed future research.

8. Concluding remarks

The influential role of crude oil fluctuations upon individual financial asset segments (such as equity, bonds, and precious metals, among others) is well-established in the existing literature. While those studies are relevantly unwinding the segment-specific vulnerabilities of financial markets with respect to oil shocks, however, not sufficient to decipher the overall standing of the market. Thus, Chen et al. (2014) suggest FSI as an appropriate measure of expectations of financial market losses induced by macroeconomic uncertainties such as oil shocks. Thus, this study examines the relationship between oil volatility (proxied by OVX) with respect to composite and categorical indicators of financial stress using a continuous wavelet transformation framework, which is seldom in the existing literature.

The outcome of the study indicates that there exists a co-movement between oil volatility and financial stress, mainly around periods of economic turbulence. The patterns and strength of co-movement are time-varying and episodic. Further, the impact of OVX varies across the

categories and nature of financial stress. Additionally, the direction of the relationship is mainly positive, and the lead-lag relationship, in most instances, reveals that OVX tends to drive the significant co-movement. In terms of causality, it is observed that they are mostly bi-directional, as consistent with Das et al. (2018b); however, relatively stronger causalities are transmitted from OVX to the stress components. The zones of causal transmission also correspond to the phases of economic instabilities such as the GFC, oil oversupply shock and COVID-19. To attest to the findings further, the OVX and stress indicators are decomposed into positive and negative values as represented by the phases. While the positive values indicate a state of distress, the negative values represent a state of tranquillity. The results suggest that the causalities are mainly existent in the state of distress than otherwise. Thus, the relationship between OVX and stress must be given attention, especially during the phase of economic turbulence.

The findings of this study could be useful to several policymakers, such as energy economists, financial analysts and oil production and supply regulatory cartels. The potential arenas of financial vulnerabilities expected to stem from oil volatility (originating from production cuts or sluggish demand) could be projected, and remedial measures can be sought to mitigate the adverse shocks. Besides, the findings are equally relevant for the investors and other market participants to anticipate the potential impacts of OVX on the different classes of stress.

Therefore, portfolio choices and diversification strategies may be framed according to the anticipated risk. In addition, understanding the persistence of the association indicated by the frequency dimension in the wavelet maps may aid in predicting the time lag of information diffusion. This also emphasizes the use of wavelet-based techniques. As a future course of study, one potential area could be the investigation of co-movement and causal transmission of structural crude oil shocks with respect to the various stress indicators in a wavelet framework. Such an ensuing study may deepen the understanding of this sphere of literature. In addition, as stated earlier, the underlying reason for causal transmission from US stress to oil market uncertainties may also be examined.

Note: The *White* and *Yellow* contours in sub-figures (a) and (b) represent the statistical significance at 5% and 10%, respectively. The significance levels are derived on 3000 Monte-Carlo simulation draws estimated on ARMA (1,1) null of no statistical significance. The COI is depicted by the *green* line, which demarcates the zones affected by edge effects. The scale has been transformed to a period for the Morlet wavelet function. Using $\omega_0 = 6$ for the optimal balance (Torrence and Compo, 1998), we have $Ft = 1.033$. s.

Appendix A. Supplementary data

Supplementary data to this article can be found online at <https://doi.org/10.1016/j.eneco.2022.106388>.

References

- Aguiar-Conraria, L., Azevedo, N., Soares, M.J., 2008. Using wavelets to decompose the time-frequency effects of monetary policy. *Phys. A Stat. Mech. its Appl.* 387, 2863–2878.
- Ahmed, A.D., Huo, R., 2021. Volatility transmissions across international oil market, commodity futures and stock markets: empirical evidence from China. *Energy Econ.* 93, 104741.
- Alam, M.S., Shahzad, S.J.H., Ferrer, R., 2019. Causal flows between oil and forex markets using high-frequency data: asymmetries from good and bad volatility. *Energy Econ.* 84, 104513.
- Albullescu, C.T., Ajmi, A.N., 2021. Oil price and US dollar exchange rate: change detection of bi-directional causal impact. *Energy Econ.* 100, 105385.
- Apostolakis, G.N., Floros, C., Gkillas, K., Wohar, M., 2021. Financial stress, economic policy uncertainty, and oil price uncertainty. *Energy Econ.* 104, 105686.
- Arora, V., Vamvakidis, A., 2006. The impact of U.S. economic growth on the rest of the world: how much does it matter? *J. Econ. Integr.* 21 (1), 21–39.
- Arouri, M.E.H., Rault, C., 2012. Oil prices and stock markets in GCC countries: empirical evidence from panel analysis. *Int. J. Financ. Econ.* 17, 242–253.
- Arouri, M.E.H., Jouini, J., Nguyen, D.K., 2011. Volatility spillovers between oil prices and stock sector returns: implications for portfolio management. *J. Int. Money Financ.* 30, 1387–1405.
- Attems, B., Kapper, D., Lam, E., 2015. Do exchange rates respond asymmetrically to shocks in the crude oil market? *Energy Econ.* 49, 227–238.
- Basher, S.A., Haug, A.A., Sadowsky, P., 2012. Oil prices, exchange rates and emerging stock markets. *Energy Econ.* 34, 227–240.
- Basta, M., Molnár, P., 2018. Oil market volatility and stock market volatility. *Financ. Res. Lett.* 26, 204–214.
- Baur, D.G., Lucey, B.M., 2010. Is gold a hedge or a safe haven? An analysis of stocks, bonds and gold. *Financ. Rev.* 45, 217–229.
- Beckmann, J., Czudaj, R.L., Arora, V., 2020. The relationship between oil prices and exchange rates: revisiting theory and evidence. *Energy Econ.* 88, 104772.
- Bekaert, G., Ehrmann, M., Fratzscher, M., Mehl, A., 2014. The global crisis and equity market contagion. *J. Financ.* 69, 2597–2649.
- Bianchi, R.J., Fan, J.H., Todorova, N., 2020. Financialization and de-financialization of commodity futures: a quantile regression approach. *Int. Rev. Financ. Anal.* 68, 101451.
- Bodenstein, M., Guerrieri, L., Gust, C.J., 2013. Oil shocks and the zero bound on nominal interest rates. *J. Int. Money Financ.* 32, 941–967.
- Boldanov, R., Degiannakis, S., Filis, G., 2016. Time-varying correlation between oil and stock market volatilities: evidence from oil-importing and oil-exporting countries. *Int. Rev. Financ. Anal.* 48, 209–220.
- Bouri, E., 2015a. Oil volatility shocks and the stock markets of oil-importing MENA economies: a tale from the financial crisis. *Energy Econ.* 51, 590–598.
- Bouri, E., 2015b. Return and volatility linkages between oil prices and the Lebanese stock market in crisis periods. *Energy* 89, 365–371.
- Bouri, E., Jain, A., Biswal, P.C., Roubaud, D., 2017. Cointegration and nonlinear causality amongst gold, oil, and the Indian stock market: evidence from implied volatility indices. *Res. Policy* 52, 201–206.
- Bouri, E., Shahzad, S.J.H., Raza, N., Roubaud, D., 2018. Oil volatility and sovereign risk of BRICS. *Energy Econ.* 70, 258–269.
- Charlot, P., Marimoutou, V., 2014. On the relationship between the prices of oil and the precious metals: revisiting with a multivariate regime-switching decision tree. *Energy Econ.* 44, 456–467.
- Chen, W., Hamori, S., Kinkyo, T., 2014. Macroeconomic impacts of oil prices and underlying financial shocks. *J. Int. Financ. Mark. Inst. Money* 29, 1–12.
- Corbet, S., Goodell, J.W., Güney, S., 2020. Co-movements and spillovers of oil and renewable firms under extreme conditions: new evidence from negative WTI prices during COVID-19. *Energy Econ.* 92, 104978.
- Cunado, J., de Gracia, F.P., 2014. Oil price shocks and stock market returns: evidence for some European countries. *Energy Econ.* 42, 365–377.
- Dai, Z., Kang, J., 2021. Bond yield and crude oil prices predictability. *Energy Econ.* 97, 105205.
- Das, D., Dutta, A., Jana, R.K., Ghosh, I., 2022a. The asymmetric impact of oil price uncertainty on emerging market financial stress: a quantile regression approach. *Int. J. Financ. Econ.* <https://doi.org/10.1002/jife.2651>.
- Das, D., Kannadhasan, M., 2020. The asymmetric oil price and policy uncertainty shock exposure of emerging market sectoral equity returns: a quantile regression approach. *Int. Rev. Econ. Financ.* 69, 563–581.
- Das, D., Kumar, S.B., 2018. International economic policy uncertainty and stock prices revisited: multiple and partial wavelet approach. *Econ. Lett.* 164 <https://doi.org/10.1016/j.econlet.2018.01.013>.
- Das, D., Kannadhasan, M., Al-Yahyaee, K.H., Yoon, S.M., 2018a. A wavelet analysis of co-movements in Asian gold markets. *Phys. A Stat. Mech. its Appl.* 492, 192–206. <https://doi.org/10.1016/j.physa.2017.09.061>.
- Das, D., Kumar, S.B., Tiwari, A.K., Shahbaz, M., Hasim, H.M., 2018b. On the relationship of gold, crude oil, stocks with financial stress: a causality-in-quantiles approach. *Financ. Res. Lett.* 27, 169–174. <https://doi.org/10.1016/j.frl.2018.02.030>.
- Das, D., Kannadhasan, M., Bhattacharya, M., 2022b. Oil price shocks and emerging stock markets revisited. *International Journal of Emerging Markets* 17 (6), 1583–1614. <https://doi.org/10.1108/IJOM-02-2020-0134>.
- Das, D., Le Roux, C.L., Jana, R.K., Dutta, A., 2020. Does bitcoin hedge crude oil implied volatility and structural shocks? A comparison with gold, commodity and the US Dollar. *Financ. Res. Lett.* 36, 1–11. <https://doi.org/10.1016/j.frl.2019.101335>.
- Dickey, D.A., Fuller, W.A., 1979. Distribution of the estimators for autoregressive time series with a unit root. *J. Am. Stat. Assoc.* 74, 427–431.
- Diebold, F.X., Yilmaz, K., 2009. Measuring financial asset return and volatility spillovers, with application to global equity markets. *Econ. J.* 119, 158–171.
- Diebold, F.X., Yilmaz, K., 2012. Better to give than to receive: predictive directional measurement of volatility spillovers. *Int. J. Forecast.* 28, 57–66.
- Diebold, F.X., Yilmaz, K., 2014. On the network topology of variance decompositions: measuring the connectedness of financial firms. *J. Econ.* 182, 119–134.
- Dutta, A., 2017. Oil price uncertainty and clean energy stock returns: new evidence from crude oil volatility index. *J. Clean. Prod.* 164, 1157–1166.
- Dutta, A., 2018. Oil and energy sector stock markets: an analysis of implied volatility indexes. *J. Multinatl. Financ. Manag.* 44, 61–68.
- Dutta, A., Nikkinen, J., Rothovius, T., 2017. Impact of oil price uncertainty on Middle East and African stock markets. *Energy* 123, 189–197.
- Dutta, A., Das, D., Jana, R.K., Vo, X.V., 2020. COVID-19 and oil market crash: revisiting the safe haven property of gold and bitcoin. *Res. Policy* 69, 101816.
- Dutta, A., Bouri, E., Saeed, T., Vo, X.V., 2021. Crude oil volatility and the biodiesel feedstock market in Malaysia during the 2014 oil price decline and the COVID-19 outbreak. *Fuel* 292, 120221.
- El-Sharif, I., Brown, D., Burton, B., Nixon, B., Russell, A., 2005. Evidence on the nature and extent of the relationship between oil prices and equity values in the UK. *Energy Econ.* 27, 819–830.
- Gallegati, M., 2012. A wavelet-based approach to test for financial market contagion. *Comput. Stat. Data Anal.* 56, 3491–3497.
- Geweke, J., 1982. Measurement of linear dependence and feedback between multiple time series. *J. Am. Stat. Assoc.* 77, 304–313.
- Gkillas, K., Gupta, R., Pierdzioch, C., 2020. Forecasting realized oil-price volatility: the role of financial stress and asymmetric loss. *J. Int. Money Financ.* 104, 102137.
- Gong, X., Lin, B., 2018a. The incremental information content of investor fear gauge for volatility forecasting in the crude oil futures market. *Energy Econ.* 74, 370–386.
- Gong, X., Lin, B., 2018b. Time-varying effects of oil supply and demand shocks on China's macro-economy. *Energy* 149, 424–437.
- Gong, X., Liu, Y., Wang, X., 2021. Dynamic volatility spillovers across oil and natural gas futures markets based on a time-varying spillover method. *Int. Rev. Financ. Anal.* 76, 101790.
- Granger, C.W.J., 1969. Investigating causal relations by econometric models and cross-spectral methods. *Econom. J. Econom. Soc.* 424–438.
- Gupta, R., Kanda, P., Tiwari, A.K., Wohar, M.E., 2019. Time-varying predictability of oil market movements over a century of data: the role of US financial stress. *North Am. J. Econ. Financ.* 50, 100994.
- Hammoudeh, S., 1988. The oil market and its impact on the economic development of the oil-exporting countries. *J. Energy Dev.* 297–324.
- Heathcote, J., Perri, F., 2003. Why has the US economy become less correlated with the rest of the world? *Am. Econ. Rev.* 93 (2), 63–69.
- Illing, M., Liu, Y., 2006. Measuring financial stress in a developed country: an application to Canada. *J. Financ. Stab.* 2, 243–265.
- Ioannidis, C., Ka, K., 2018. The impact of oil price shocks on the term structure of interest rates. *Energy Econ.* 72, 601–620.
- Jiang, Z., Yoon, S.-M., 2020. Dynamic co-movement between oil and stock markets in oil-importing and oil-exporting countries: two types of wavelet analysis. *Energy Econ.* 90, 104835.
- Jones, C.M., Kaul, G., 1996. Oil and the stock markets. *J. Financ.* 51, 463–491.

- Kang, S.H., Tiwari, A.K., Albulescu, C.T., Yoon, S.-M., 2019. Time-frequency co-movements between the largest nonferrous metal futures markets. *Res. Policy* 61, 393–398.
- Kang, W., Ratti, R.A., Yoon, K.H., 2014. The impact of oil price shocks on US bond market returns. *Energy Econ.* 44, 248–258.
- Kilian, L., 2009. Not all oil price shocks are alike: disentangling demand and supply shocks in the crude oil market. *Am. Econ. Rev.* 99, 1053–1069.
- Kilian, L., Park, C., 2009. The impact of oil price shocks on the US stock market. *Int. Econ. Rev. (Philadelphia)* 50, 1267–1287.
- Kivimäki, J., Nikkinen, J., Piljak, V., Rothovius, T., 2014. The co-movement dynamics of European frontier stock markets. *Eur. Financ. Manag.* 20, 574–595.
- Kunkler, M., MacDonald, R., 2019. The multilateral relationship between oil and G10 currencies. *Energy Econ.* 78, 444–453.
- Kwiatkowski, D., Phillips, P.C.B., Schmidt, P., Shin, Y., 1992. Testing the null hypothesis of stationarity against the alternative of a unit root. *J. Econ.* 54, 159–178.
- Lee, C.-C., Zeng, J.-H., 2011. The impact of oil price shocks on stock market activities: asymmetric effect with quantile regression. *Math. Comput. Simul.* 81, 1910–1920.
- Lee, Chi-Chuan, Lee, Chien-Chiang, 2019. Oil price shocks and Chinese banking performance: do country risks matter? *Energy Econ.* 77, 46–53.
- Liu, M.-L., Ji, Q., Fan, Y., 2013. How does oil market uncertainty interact with other markets? An empirical analysis of implied volatility index. *Energy* 55, 860–868.
- Liu, R., Chen, J., Wen, F., 2021. The nonlinear effect of oil price shocks on financial stress: evidence from China. *North Am. J. Econ. Financ.* 55, 101317.
- Lu, X., Ma, F., Wang, Jiqian, Wang, Jianqiong, 2020. Examining the predictive information of CBOE OVX on China's oil futures volatility: Evidence from MS-MIDAS models. *Energy* 212, 118743.
- Ma, Y.-R., Zhang, D., Ji, Q., Pan, J., 2019. Spillovers between oil and stock returns in the US energy sector: does idiosyncratic information matter? *Energy Econ.* 81, 536–544.
- Madaleno, M., Pinho, C., 2014. Wavelet dynamics for oil-stock world interactions. *Energy Econ.* 45, 120–133.
- Maghayreh, A.I., Awartani, B., Bouri, E., 2016. The directional volatility connectedness between crude oil and equity markets: new evidence from implied volatility indexes. *Energy Econ.* 57, 78–93.
- Maitra, D., Guhathakurta, K., Kang, S.H., 2021. The good, the bad and the ugly relation between oil and commodities: an analysis of asymmetric volatility connectedness and portfolio implications. *Energy Econ.* 94, 105061.
- Malik, F., Ewing, B.T., 2009. Volatility transmission between oil prices and equity sector returns. *Int. Rev. Financ. Anal.* 3, 95–100.
- Malik, F., Hammoudeh, S., 2007. Shock and volatility transmission in the oil, US and gulf equity markets. *Int. Rev. Econ. Financ.* 16, 357–368.
- Mokni, K., 2020. A dynamic quantile regression model for the relationship between oil price and stock markets in oil-importing and oil-exporting countries. *Energy* 213, 118639.
- Narayan, P.K., Narayan, S., 2010. Modelling the impact of oil prices on Vietnam's stock prices. *Appl. Energy* 87, 356–361.
- Nazlioglu, S., Soytas, U., Gupta, R., 2015. Oil prices and financial stress: a volatility spillover analysis. *Energy Policy* 82, 278–288.
- Olayeni, O.R., 2016. Causality in continuous wavelet transform without spectral matrix factorization: theory and application. *Comput. Econ.* 47, 321–340.
- Pang, D., Ma, F., Wahab, M.I.M., Zhu, B., 2021. Financial stress and oil market volatility: new evidence. *Appl. Econ. Lett.* 1–6.
- Percival, D.B., Mofjeld, H.O., 1997. Analysis of subtidal coastal sea level fluctuations using wavelets. *J. Am. Stat. Assoc.* 92, 868–880.
- Percival, D.B., Walden, A.T., 2000. *Wavelet Methods for Time Series Analysis*. Cambridge University Press.
- Phillips, P.C.B., Perron, P., 1988. Testing for a unit root in time series regression. *Biometrika* 75, 335–346.
- Püttmann, L., 2018. Patterns of Panic: Financial Crisis Language in Historical Newspapers. Available SSRN 3156287.
- Ready, R.C., 2018. Oil prices and the stock market. *Rev. Financ.* 22, 155–176.
- Reboredo, J.C., Rivera-Castro, M.A., 2014. Wavelet-based evidence of the impact of oil prices on stock returns. *Int. Rev. Econ. Financ.* 29, 145–176.
- Reboredo, J.C., Uddin, G.S., 2016. Do financial stress and policy uncertainty have an impact on the energy and metals markets? A quantile regression approach. *Int. Rev. Econ. Financ.* 43, 284–298.
- Reboredo, J.C., Rivera-Castro, M.A., Ugolini, A., 2017. Wavelet-based test of co-movement and causality between oil and renewable energy stock prices. *Energy Econ.* 61, 241–252.
- Rua, A., 2013. Worldwide synchronization since the nineteenth century: a wavelet-based view. *Appl. Econ. Lett.* 20, 773–776.
- Sadorsky, P., 1999. Oil price shocks and stock market activity. *Energy Econ.* 21, 449–469.
- Saif-Alyousfi, A.Y.H., Saha, A., Md-Rus, R., Taufil-Mohd, K.N., 2020. Do oil and gas price shocks have an impact on bank performance? *J. Commod. Mark.* 100147.
- Szczygielski, J.J., Brzeszczynski, J., Charteris, A., Bwanya, P.R., 2021. The COVID-19 storm and the energy sector: the impact and role of uncertainty. *Energy Econ.* 109, 105258.
- Tiwari, A.K., Albulescu, C.T., 2016. Oil price and exchange rate in India: fresh evidence from continuous wavelet approach and asymmetric, multi-horizon Granger-causality tests. *Appl. Energy* 179, 272–283.
- Tiwari, A.K., Mutascu, M.I., Albulescu, C.T., 2013. The influence of the international oil prices on the real effective exchange rate in Romania in a wavelet transform framework. *Energy Econ.* 40, 714–733.
- Tiwari, A.K., Bhattacharyya, M., Das, D., Shahbaz, M., 2018a. Output and stock prices: new evidence from the robust wavelet approach. *Financ. Res. Lett.* 27, 154–160. <https://doi.org/10.1016/j.frl.2018.02.005>.
- Tiwari, A.K., Jena, S.K., Mitra, A., Yoon, S.-M., 2018b. Impact of oil price risk on sectoral equity markets: implications on portfolio management. *Energy Econ.* 72, 120–134.
- Torrence, C., Compo, G.P., 1998. A practical guide to wavelet analysis. *Bull. Am. Meteorol. Soc.* 79, 61–78.
- Tule, M.K., Ndako, U.B., Onipepe, S.F., 2017. Oil price shocks and volatility spillovers in the Nigerian sovereign bond market. *Rev. Financ. Econ.* 35, 57–65.
- Uddin, G.S., Rahman, M.L., Shahzad, S.J.H., Rehman, M.U., 2018. Supply and demand driven oil price changes and their non-linear impact on precious metal returns: a Markov regime switching approach. *Energy Econ.* 73, 108–121.
- Umar, Z., Jareno, F., Escribano, A., 2021. Oil price shocks and the return and volatility spillover between industrial and precious metals. *Energy Econ.* 99, 105291.
- Wan, J.-Y., Kao, C.-W., 2015. Interactions between oil and financial markets—do conditions of financial stress matter? *Energy Econ.* 52, 160–175.
- Wang, H., Li, S., 2021. Asymmetric volatility spillovers between crude oil and China's financial markets. *Energy* 233, 121168.
- Wang, Y., Wei, Y., Wu, C., Yin, L., 2018. Oil and the short-term predictability of stock return volatility. *J. Empir. Financ.* 47, 90–104.
- Xiao, J., Zhou, M., Wen, Fengming, Wen, Fenghua, 2018. Asymmetric impacts of oil price uncertainty on Chinese stock returns under different market conditions: evidence from oil volatility index. *Energy Econ.* 74, 777–786.
- Xiao, J., Hu, C., Ouyang, G., Wen, F., 2019. Impacts of oil implied volatility shocks on stock implied volatility in China: empirical evidence from a quantile regression approach. *Energy Econ.* 80, 297–309.
- Xie, Q., Wu, H., Ma, Y., 2021. Refining the asymmetric impacts of oil price uncertainty on Chinese stock returns based on a semiparametric additive quantile regression analysis. *Energy Econ.* 102, 105495.
- You, W., Guo, Y., Zhu, H., Tang, Y., 2017. Oil price shocks, economic policy uncertainty and industry stock returns in China: asymmetric effects with quantile regression. *Energy Econ.* 68, 1–18.